Manuscript type: Research Article

Title: The developmental gene *disco* regulates diel-niche evolution in adult moths

Authors: Yash Sondhi1[1,2] (ORCID:0000-0002-7704-3944), Rebeccah L. Messcher[2], Anthony J. Bellantuano[1], Caroline G. Storer[2], Scott D. Cinel[2], R. Keating Godfrey[2], Deborah Glass[4], Ryan A. St Laurent[2,6], Chris A. Hamilton[5], Chandra Earl[7], Colin J. Brislawn[2], Ian J. Kitching[4], Seth M. Bybee[3], Jamie C. Theobald[1], Akito Y. Kawahara[2]

Author Affiliation:

[1]Department of Biology, Florida International University, Miami FL 33174 USA

[2]McGuire Center for Lepidoptera and Biodiversity, Florida Museum of Natural History, University of Florida, Gainesville, FL 32611 USA

[3]Department of Biology, Monte L. Bean Museum, Brigham Young University, 4102 Life Science Building, Provo, UT 84602, USA

[4]Natural History Museum, Cromwell Road, London SW7 5BD, UK.

[5]Department of Entomology, Plant Pathology & Nematology, University of Idaho, Moscow, ID 83844, USA

[6]Department of Entomology, Smithsonian Institution, National Museum of Natural History, Washington, D.C., U.S.A

[7]Bernice P. Bishop Museum, Honolulu, HI 96817, USA

Corresponding author: Yash Sondhi, yashsondhi@gmail.com

Keywords: circadian; development, diel-niche; gene expression; insects; Lepidoptera; light cycle; RNA-seq transcriptome, transcription factor

Significance: Insects have been longstanding models for understanding circadian and sensory biology. The diversity of diel-activity patterns of insects is tremendous, yet our understanding of the genetic and evolutionary processes leading to this diversity is limited. Light environment is a powerful circadian entrainer that drives diel-niche and sensory evolution. To investigate the evolutionary impact of highly shifted light environments on animals with otherwise similar ecologies, we compared gene expression in closely related day- and night-active wild silkmoths.

Genes linked to eye development, neural plasticity and energy cellular maintenance showed expression patterns linked to diel activity. Notably, *disco*, a gene encoding a zinc finger transcription factor involved in fly (*Drosophila melanogaster)* optic lobe and antennal development in the pupa, shows robust adult circadian mRNA cycling in moth heads, is highly conserved in moths, and has additional zinc-finger domains with specific nocturnal and diurnal mutations. We hypothesize that *disco* may contribute to diversification of adult diel-activity patterns in moths.

Abstract:

Circadian rhythms drive many biological patterns, such as activity periods. The temporal partitioning that results can reduce predation, minimize competition, or enable new resource utilization. It can also drive the evolution of sensory systems, such as the highly specialized antennae with which male moths find mates, and the visual specializations with which butterflies escape from birds. However, the mechanisms that underlie such niche-shift adaptations are poorly understood. Many model organisms in circadian biology are too distantly related from one another to elucidate the genetic drivers of diel-niche transitions. To address this, we examined gene expression patterns between two closely related wild silk moth species (Saturniidae), that utilize similar host plants and habitats, but have undergone temporal niche divergence. We found 200-700 differentially expressed genes, including day upregulation in eye development and visual processing genes, and night upregulation of antennal and olfactory brain development genes. We also found clusters of circadian, sensory, and brain development genes co-expressing with diel-activity. Eight genes showed a clear and statistically significant correlation between expression and diel activity in both species, and were involved in vision, olfaction, brain development, neural plasticity, energy utilization, and cellular maintenance. Disconnected (*disco)*, a zinc-finger transcription factor involved in antennal development, circadian activity, and optic lobe brain development in flies, was repeatedly recovered in multiple analyses. While *disco* mutants have circadian arrhythmia, most studies have attributed this to improper clock neuron development, and not directly to adult circadian maintenance. Comparing predicted 3D protein structure across moth (*Bombyx mori)* and fly (*Drosophila melanogaster)* genetic models revealed *disco* has likely retained its developmental function with a conserved zinc finger domain, but it has also likely gained novel functional zinc

finger domains, highly conserved in moths, but absent in *D. melanogaster.* These regions had several mutations between nocturnal and diurnal study species that co-occur with higher levels of predicted phosphorylation sites. Together, robust circadian gene expression, functional nocturnal and diurnal mutations with high phosphorylation, structural and sequence conservation, leads us to hypothesize that *disco* may be a master regulator contributing to the diversification of adult diel-activity patterns in adult moths.

Introduction

Circadian rhythms regulate many biological processes, including day-night activity patterns. Research to date has explored genes, circuits, and environmental cues mostly in the context of control within a single organism (1, 2). Diel-niche stems from the concept of temporal partitioning of activity periods, driven by the variation in resources, temperature, light level, or predation, across the day (3–6). Periods are often binned into three distinct groups: diurnal (day active), nocturnal (night active), or crepuscular (active at dusk, dawn, or both), and although this is useful for comparative analysis, it is often an overgeneralization (7–11), and the evolution of diverse diel-niches across organisms (7, 11–15) is poorly understood (16–19).

Several studies have documented sensory adaptation accompanying evolutionary diel-niche transitions in mammals, birds, and insects (8, 18, 20, 21). Specific examples include colour vision gene expansions in diurnal moths (22, 23), improved olfactory senses in dark-bred flies (24), and the evolution of hearing organs in nocturnal butterflies (25). Comparisons of circadian genes across model organisms catalogue variation at long evolutionary timescales and highlight conserved elements (26, 27), but diel switches can occur over short timescales (28), and distantly related species provide less insight into mechanisms that enable faster switches. Moths and butterflies (Lepidoptera) are an ideal group to address this, as their evolutionary history is well known and there are many diel-niche switches, often between closely related species (7, 29). They are also one of the few insect groups, outside of *Drosophila*, in which both sensory and circadian genes have been characterized (23, 30–35).

Wild silk moths (Saturniidae) are important models for understanding chronobiology, with seminal experiments confirming the brain functions as the primary circadian control (36, 37). While most are nocturnal, many fly during the day, and temporal niche switches may function as a

92 mechanism for reproductive isolation in sympatric species (38, 39). Saturniid phylogeny is relatively
93 well known, and there are several annotated genomes, chromosomal maps. Furthermore, they belong
94 to the superfamily Bombycoidea, which includes the domesticated silk moth, *Bombyx mori*, a key
95 biological model organism serving as a reference taxon for comparative genomic studies (32, 40–43).
96 Saturniids such as *Antheraea* are of major importance to the silk industry, and they have a well-
97 resolved taxonomy and well-documented life histories (38, 44–46). Despite this, the genetic elements
98 that control day-night activity and diel-niche evolution, in this group and insects in general, remain
99 largely unknown (28, 37).
100 We used RNA-Seq to characterize expression patterns during peaks and troughs (midday and
101 midnight) across two closely related wild silkmoths: the diurnal *Anisota pellucida*, and nocturnal
102 *Dryocampa rubicunda*. They are sister genera, feeding on large deciduous trees in the temperate
103 forests in Eastern North America, with a recent divergence in temporal niche ~3.8 Mya (47). We
104 sequenced head tissue at different time periods to identify expression in sensory, circadian, and
105 neural genes that correlate with diel activity. Expression in eight genes clearly and significantly
106 correlates with diel activity, with functions in vision, olfaction, brain development, neural plasticity,
107 energy utilization, and cellular maintenance. Of these, a single gene emerges consistently across
108 analyses: *disco*, which encodes a zinc-finger transcription factor. In moths, it has likely retained
109 functions also found in flies (eye and brain development during the pupal stage) through a conserved
110 zinc finger domain. But it has also gained an extra zinc-finger domain, surrounded by phosphorylated
111 sites and with mutations in both nocturnal and diurnal species, which may contribute to adult moth
112 circadian regulation.
113

114 **Results**

115 We compared gene expression across two wild silk moth species, *Anisota pellucida* and *Dryocampa*
116 *rubicunda*, whose males are diurnal and nocturnal, respectively (Fig. 1, Table 1). We generated head
117 (eyes, brain) transcriptomes from moths collected and flash frozen at midday and midnight, referred
118 to as 'day' and 'night' hereafter. Using multiple programs to assemble high-quality *de novo*
119 assemblies (Table 2), we characterized the level of gene (mRNA) expression with quasi-read
120 mapping, which can be used to correlate protein expression (48).

121

122 ***Day-night gene expression patterns switch between nocturnal and diurnal species***

123 We found 350 & 393 significantly differentially expressed genes (DEGs) when comparing day and
124 night treatments for each species (Table 3, Fig. 2A). *Anisota* had more day-upregulated genes (56%)
125 and *Dryocampa* was slightly more night-upregulated (53%). In order to compare DEG sets between
126 species, we mapped our DEGs to *Bombyx mori* orthologs using the Orthofinder software (49)
127 (Supplementary Data 1). Approximately 60% of DEGs from each species had identifiable orthologs
128 in *B. mori* (Table 3), and only a small number of DEGs (6-8 genes) overlapped between both species
129 (Fig. 2B). We also replicated this analysis using other software to assure that our results were robust,
130 despite different normalization methods (50). With DESeq2, we found 498 & 697 DEGs (Fig. 2C,
131 Table 3, Supplementary Data 2), with similar *Bombyx* annotation rates (61%), although the
132 proportion of day upregulated genes increased considerably in the *Anisota* (79%) compared to being
133 more even split in *Dryocampa* (50%) (Table 3). The total number of overlapping genes increased
134 (19-26, Fig. 2D) when using DESeq2. A comparison of the two methods revealed that 174 and 216
135 genes were shared between *Anisota* and *Dryocampa*, respectively.

136

137 ***Divergently expressed genes are linked to brain optic lobe, antennal and neural development***

138 To identify important regulators involved in diel-niche evolution, we applied two filtering criteria to
139 our gene expression data. First, we selected genes that exhibited highly significant differential
140 expression in both species. Second, we focused on genes that displayed upregulation patterns
141 consistent with the natural diel-activity of each species. Our rationale was that this subset of genes
142 was more likely to contain key regulators. To compare DEG overlap between the two species, we
143 grouped the transcripts to their matching orthologs from *Bombyx mori*; if two transcripts from
144 different species mapped to the same ortholog, we treated them as being the same. This allowed us to
145 examine overlapping genes between the species to see if any genes switched fold-change sign from
146 positive to negative or vice versa. (Fig. 2, Supplementary Data 3). We found 51 overlapping DEG
147 transcripts that mapped to 28 unique *Bombyx* genes. Nine genes showed flipped patterns of
148 expression between the two species, and eight of them coincided with known diel activity patterns
149 (Table 7). Examining gene ontology (GO) annotations and comparing orthologs from flybase
150 (https://flybase.org/), we found genes linked to optic lobe and antennal development (*disco*),

151 locomotion and energy use (*SLC2A6, SLC17A5*), brain and neural development (*TUBG1*) and other
152 essential biological processes like transcription, ribosomal translation, protein processing,
153 mitochondrial maintenance (*RpS4, PARL, Mrps5*) and wound response (*PRP2*) (Table 7, Fig. 2B, D).
154 Of these, only *disco* was recovered with both methods.
155
156 ***Gene network analysis identifies diel activity and species-specific co-expressed clusters***
157 Identifying highly expressed genes helps understand which genes are activated during particular
158 biological processes. However, determining only those that are highly expressed can often overlook
159 genes with important biological functions (51). We examined co-expressed genes that may be
160 correlated with diel-niche or RNA collection time. We used WGCNA, a weighted correlation
161 network analysis tool to cluster genes together based on their normalized counts (52). After
162 examining co-expression patterns for each species separately, we found two modules in each species
163 that clustered with day-night treatment (cluster-*grey60* and cluster-*tan*) (Fig. S6, Supplementary data
164 4). Since we were interested in species-specific differences, we reran analyses and combined reads
165 from *Anisota* and *Dryocampa,* using only normalized counts for genes that had valid *Bombyx*
166 annotations for both species. This approach narrowed our focus to 2000 genes. Among these, we
167 discovered two clusters (cluster-blue and cluster-turquoise) consisting of 50 genes each that exhibited
168 different expression patterns across species (Fig. 4).
169
170 ***GO enrichment of photoperiodism, circadian control, muscle and neural growth genes***
171 We used a gene enrichment analysis to determine if gene ontology (GO) terms were significantly
172 overrepresented in the DEG and WGCNA sets compared to the appropriate background of GO terms.
173 Using TopGo, which allows custom gene sets, we found an overrepresentation of genes involved in
174 several biological functions (Supplementary Table 1). Those that seemed significant for diel-niche
175 and vision were 'response to stimulus' and 'smooth muscle control', as well as folic acid serine,
176 glycine and retinoic acid metabolism. We also used ShinyGo to examine WGCNA clusters
177 (Supplementary Data 5). We matched orthologous genes in the less duplicated, filtered
178 transcriptomes to obtain identifications of the most related *Bombyx* genes (Table 4). We examined
179 the enrichment of both tan and grey60 modules, listing the non-redundant terms using ReviGo (Fig.
180 S7, Supplementary Table 2, 3). Gene clusters that co-expressed in the same direction together in the

181 day and night treatments of both species included photoperiodism, circadian control, negative
182 phototaxis and nervous system development. We next checked for the enrichment of the modules that
183 showed species-specific patterns (blue and turquoise, Fig. S8, Supplementary Table 2). These
184 included genes involved in muscle proliferation and nerve growth, neural signaling, glycolysis,
185 oxidative stress response, and basic cellular functioning such as protein processing and
186 transcriptional regulation.

187 ***Day upregulation of vision genes in the diurnal moth***

188 Since both EdgeR and DESeq2 analyses use different normalization methods and statistical model
189 assumptions (50, 53), we repeated enrichment analyses by combining datasets and examining genes
190 that appeared in both analyses. For the *Anisota,* we tested over-enrichment of a smaller subset (FC ≤
191 -5) of diurnally highly upregulated genes (Fig. 3, Table 5). We found gene enrichment for visual
192 perception, excretion regulation, negative gravitaxis, synaptic plasticity, along with genes associated
193 with other biological processes, such as RNA interference, endopeptidase activity and endocytosis. A
194 reduction in stringency (FC ≤- 2) did not alter results considerably (Fig. S4). Night-upregulated
195 genes (FC ≥ 2) included ocellar pigment genes, eye-photoreceptor cell development, snRNA
196 processing, post embryonic development and neurotransmitter secretion, among a host of other
197 processes that may be required for growth, development and metabolism (wnt signaling,
198 tricarboxylic acid cycle, and cellular response to insulin, glucose transport) (Fig. S4).
199

200 ***Night upregulation of antennal and olfactory brain regions mushroom development genes***

201 We repeated the same analyses for *Dryocampa* and tested highly nocturnally upregulated genes (FC ≥ 5).
202 Our results show upregulation in genes known to be associated with mushroom body development,
203 locomotor rhythm, synaptic growth, energy utilization (Sialin transport) and mitochondrial translation
204 (Fig. 3B, Table 6). A reduction in stringency (|FC| ≥ 2) showed entrainment of the clock cycle, and
205 antennal development genes. Genes associated with innate immune response, DNA repair, cell division,
206 histone acetylation, circadian rhythm, retinoid cycle were upregulated during the day, possibly indicating
207 a period of cellular repair during a time when these moths are inactive (Fig. S5).
208

209 ***Key sensory, circadian, eye development and behavioral genes can drive diel-niche switches***

210 We combined results from the DEG (EdgeR and DESeq2) and gene network analyses (WGCNA) to
211 create a cumulative list of 1700 transcripts (Supplementary Data 5, 6). Focusing on genes that were
212 recovered across *Anisota* and *Dryocampa* reduced the set to 274 transcripts (Supplementary Data 7).
213 Because many transcripts had poorly annotated *Bombyx* hits, we improved annotations using the
214 program eggNog mapper (54). We tested if these genes had GO terms associated with sensory,
215 circadian, brain and neural development, or behavioral regulatory genes (Fig. 4, Table 7,
216 Supplementary Data 8). We found that several genes in each category had associated GO terms, with
217 a predominance of vision and brain development genes (Supplemental Table 4).
218
219 ***Predicted functional regions and homology patterns identified for genes of interest***
220 We examined protein and gene evolution for a set of genes which we found were of interest based on
221 results from DGE, WGCNA, GO annotations (Supplemental Table 5). In order to infer functional
222 homology from structural conservation, we downloaded high quality genomes of Bombycoidea
223 moths and relatives from Darwin Tree of Life [https://www.darwintreeoflife.org/] (Supplemental
224 Table 6). We assigned a reference protein sequence for each gene of interest from the *Bombyx mori*
225 predicted proteome. We used Orth finder to identify orthologs and filtered orthogroups containing
226 the reference sequence (49, 55). Since we had more than one gene per species, we reduced the
227 number down to a single gene by choosing the highest identity sequence relative to the *B. mori*
228 reference sequence. We also modelled the 3D structure of *B. mori* proteins and mapped the
229 evolutionary conservation onto the 3D predicted structure for proteins above a certain conservation
230 threshold (Supplementary Data 9). These analyses predict structurally and functional conserved
231 regions of proteins (Fig S9, Supplementary Data 10). We repeated this analysis with 38 insect
232 genomes (Supplemental Table 7) and mapped evolutionary conservation onto 3D protein structure
233 (Supplementary Data 9,10). We include results of evolutionary conservation analyses for two
234 regulatory candidates (*disco* and *tk*) that showed varying levels of sequence and protein evolution
235 between insects and moths (Fig. S10).
236
237 ***Modeling predicts additional functional zinc finger domains for disco in Lepidoptera***
238 *Disco* was recovered across multiple analyses. In *Drosophila melanogaster* it is known for its role in
239 eye development, important for circadian maintenance, and for leg and antennal appendage

240 formation (56–60). To determine if *disco* was conserved between moths and *Drosophila*, we
241 compared the primary sequence and 3D protein structure of *Drosophila* and *Bombyx mori*. In the
242 moth, the sequence length of *disco* was nearly double that of *Drosophila* (Fig 6A). However, a region
243 spanning over 100 amino acids was highly conserved, contained the zinc-finger domain important for
244 its function, and showed strong 3D structural conservation (Whole protein alignment RMSD(align,
245 super) = 37.833, 2.566, MatchAlign score (align, super) = 540 (2234 atoms), 333.1 (554 atoms) vs.
246 alignment of conserved region RMSD=2.699,2.566, MatchAlignScore =443(671 atoms), 351 (615)
247 atoms). This indicates the DNA binding function of *disco* has likely been conserved. However, an
248 additional ~500 amino acid region absent in *Drosophila* is highly conserved across moths, and
249 includes several regions predicted to be functional (Fig. 6A, Fig. S10). We hypothesize that *disco* has
250 a novel role in moths for diel-niche regulation. To further test this, we compared *disco* sequences
251 across *Anisota* and *Dryocampa* and found 23 mutations between them, three of which mapped to the
252 predicted functional region (Fig. 6B, Supplementary Data 10). InterProScan predicted four zinc
253 finger domains, three in this region, although the CATH-Gene3D databases prediction combined the
254 two separate domains into a single predicted domain (Fig. S11). We also found many sites (53) with
255 predicted phosphorylation potential, especially around the second zinc finger domain (18). Reducing
256 the stringency increased the total to 142, which were still enriched around the second domain.
257

258 **Discussion**

259 We identified the genetic mechanisms of diel-niche switches by examining gene expression during
260 the day and night in two closely related moth species. We used RNA-Seq to measure gene expression
261 profiles of head tissue and isolated sensory, circadian and neural processes. We found between 300
262 and 700 genes that significantly altered day night circadian expression patterns. The diurnal species
263 had enriched visual perception genes during the day and the nocturnal species had locomotor and
264 olfactory genes upregulated at night.

265 Thirty overlapping DEGs were present in both species, with some DGEs showing divergent
266 patterns of expression matching the species' diel-niche. Examining expression data with a sensitive
267 clustering analysis yielded over 170 genes that showed day-night or species specific co-expressed
268 clusters. We also used GO terms to search for genes associated with sensory, neural, or circadian
269 patterns. We found genes in each category (Supplemental Table 4) and modeled the 3D structure and

270 predicted functional regions for a subset (Supplemental Table 5). The divergently expressed gene
271 *disconnected* (*disco*) was implicated in vision, hearing, locomotion and brain development. Given the
272 multiple lines of evidence supporting the importance of this gene in regulating diurnal and nocturnal
273 activity in moths, we explored the evolution of *disco* by modeling fly and moth *disco* structures. This
274 analysis revealed novel zinc-finger conserved domains in moths, which were lacking in *Drosophila,*
275 surrounded by phosphorylated sites. Several mutations between *Anisota* and *Dryocampa* also
276 mapped to these regions, further strengthening evidence for its role in diel-niche shifts.
277
278 ***Visual and olfaction***
279 Visual systems often accompany diel and photic environment shifts (18). For example, nocturnal
280 carpenter bees have much larger facets in their eyes than their diurnal counterparts (61). Nocturnal
281 moths have higher photoreceptor light sensitivity and have neurons more suited to pooling than close
282 diurnal relatives (62). Some of these trends seem to hold across the phylogeny, with diurnal species
283 evolving more complex color visual systems, often reflected in visual opsin sequence evolution (22,
284 23). We did not find diel-expression patterns in color vision opsins, a result corroborated by a recent
285 study (22). However, we discovered a cerebral opsin (ceropsin) upregulated during the day. Ceropsin
286 has been implicated in photoperiodism and is expressed in the brain (63).
287 We also found several eye development genes (*TENM2, ANKRD17, EHD4, JAK2*),
288 phototransduction genes (*PPAP2*, *RDH11*), and retina homeostasis, eye-antennal disc development,
289 and photoreceptor cell maintenance genes (*disco, glass*) (64). Surprisingly a few visual genes, such
290 as *garnet* and *rugose* also appeared to have different isoforms present, showing both day and night
291 upregulation. *Garnet* is an eye color mutant gene in flies (65) and *rugose* is implicated in retinal
292 pattern formation (66).
293 One of the classical differences between day flying butterflies and night flying moths is that
294 butterflies have a clubbed antennae, while moths often have a sensilla-covered antenna; likely a
295 function of increased investment in olfactory sensing, similarly, there is also evidence for increased
296 investment in olfactory sensing in the brain, with relatively larger mushroom bodies in nocturnal
297 species (67, 68). In our diel gene-expression dataset, we found several olfactory genes, including
298 those involved in odorant binding (*Obp84a,Obp58b*), pheromone response (*tk*), mushroom body
299 development (*DAAM2 and DST*) and antennal development (*disco*).

300

301 ***Hearing and mechanoreception***

302 Many moths have active hearing organs, and these have evolved repeatedly across Lepidoptera (69),
303 and their use varies depending on the ecological context of the moth. Several drivers for moth
304 hearing include sexual selection and as a defense against insectivorous bats (70). The primary
305 nocturnal group of butterflies, Hedylidae, has reverted to a nocturnal niche and regained hearing
306 organs (25). Thus, although rudimentary vibrational hearing exists in some diurnal moths (71) it is
307 significantly more developed and used at broader frequency ranges at night, when light is less
308 available. While Saturniidae lack hearing organs (72) they may instead still have vibration
309 mechanosensors that can be useful in evading predation similar to those in locusts and crickets (73–
310 76). Indeed, we did find diel co-expression of several mechanosensory and ear development genes,
311 including *PI4KB, KCTD15, unc-22,* and *RhoGAP92B* (77)

312

313 ***Brain and neural rewiring***

314 Finding an upregulation of neural and brain development was expected since we sequenced head
315 transcriptomes. However, we tested gene expression two days after pupal eclosion, where
316 presumably gross structures are already developed, so it is possible these genes we found expressed
317 regulate adult plasticity. Adult neural plasticity has been showed in Lepidoptera and other insects
318 (78–80), and we recovered several genes linked to axon regeneration (*APOD*), central complex
319 development (*Ten-a, TENM2, DST, ALDH3A2, OGT*), central nervous system development (*disco*,
320 *RpL4*), and neuropeptide hormonal activity (*tk*). Several genes were specific to retinal ganglion cell
321 axon guidance (*TENM2*) and mushroom body development (*DAAM2*), leading us to speculate that
322 plasticity could occur through neural wiring and plasticity are shaping sensory adaptation. Many
323 Lepidoptera have distinct phenotypic plasticity in wing patterns and coloration in different seasons
324 (81), and there is some evidence that they also have seasonal plasticity in their behavior and foraging
325 preferences (82). Research has found Lepidoptera can override their innate preferences and learning
326 preferences for new visual and olfactory cues after eclosion (83). It is possible the diel-niche and
327 circadian rhythms too have plasticity, there are reports of some moth species like *Hyles lineata*
328 showing relatively labile diel-niches possibly driven by temperature and resources (84–86). These

329 same mechanisms allowing flexibility within a species, might be involved in diel-niche evolution
330 between species.
331
332 ***Circadian and behavioral regulators***
333 The behavioral state of an animal to engage in any activity, e.g., feeding, flight or mating, is likely a
334 function of circadian and behavioral regulators that respond to certain stimuli. We found differential
335 expression of genes involved in locomotion (*unc-22, KCTD15,Tk*) and circadian or rhythmic
336 behavior (*SREBF1/SREBF2, OGT, disco, JAK2*) in both species. We also found several key circadian
337 regulators like *per*, *tim* although they were downregulated only in *Dryocampa*. C*lock-like* or *takeout*
338 another gene under circadian control, (87) was expressed in both species, although without any
339 significant up or down regulation. *Takeout* was moderately conserved in the moths we examined, but
340 had diverged considerably among other insects, to the point where orthology searches with
341 Orthofinder failed to recover orthologs among insects. Even among *D. melanogaster*, its closest
342 homologs were *Jhbp5* and *takeout* which had 21-25% sequence identity (Supplementary Data 11).
343 Surprising, , it's 3D structure was highly conserved (RMSD (align, super) = 2.556, 2.755,
344 MatchAlign score (align, super) =199 , 642.937, Supplementary Data 11, Fig. S12), highlighting an
345 interesting example of likely functional convergence despite primary sequence divergence.
346
347 ***Energy use and general cellular maintenance***
348 In addition to the genes mentioned above, several key divergently expressed genes were involved in
349 energy utilization. This finding makes biological sense, as once activity is initiated, energy
350 mobilization and upregulation of basic cellular processes need to be maintained. Two of these genes
351 were *SLC175A/MFS10* and *SLC2A6/Tret1-1*, which encode different trehalose sugar transporters.
352 Trehalose is an important sugar present in insect hemolymph (88). Other genes found were ribosomal
353 (*RpL4, mRpS5*), golgi (*GCC*), and mitochondrial maintenance (*PARL/rho7*) along with
354 transcriptional regulation (*Spt5).*
355
356 ***Disco as putative master diel-niche regulator in adult moths***
357 Many genes that we discovered likely play a critical role in maintaining sensory shifts, but in order to
358 identify genes that might regulate upstream, we looked for genes that were: 1) expressed in both

359 species, 2) showed coincident expression patterns with respect to diel-niche, and 3) played a role in
360 sensory and neural functioning and circadian control. Only *disconnected* (*disco*) fit these criteria.
361 *Disco* is a key developmental and patterning gene, first discovered for its role in neural migration
362 from the disconnected optic lobe mutant phenotype (89). This gene is now considered an appendage
363 development gene, with a well characterized pupal role in antennal and leg distal patterning in
364 *Drosophila melanogaster (60)*. Mutants also have a disrupted circadian locomotor rhythm due to the
365 improper formation of neurons that express clock genes (90, 91). As a gene that is involved both in
366 optic lobe, antennal formation, and in neural wiring and circadian control, it is a very strong
367 candidate for driving behavioral diel-niche shifts and sensory adaptations (56, 57, 92). *Disco*
368 expression data from *B. mori* suggests strong adult head, antennal, and nucleus expression,
369 suggesting that it still acts as a transcription factor, and can regulate other genes (40).
370 *Disco* encodes the acid zinc finger transcription factor and is approximately 500 and 1000
371 amino acids in length in *Drosophila* and *B. mori,* respectively. Our modeling showed that a ~150
372 amino acid region is conserved structurally at the sequence level, and this region also contains zinc-
373 finger motifs associated with DNA binding (93). This indicates that *disco* likely has retained its DNA
374 binding and likely pupal and appendage patterning function in moths. We predicted the functional
375 regions of *disco* in *Bombyx* based on evolutionary conservation modelling, and found an additional
376 500 amino acids, absent in *Drosophila*, were predicted to be functional (conserved and exposed).
377 Domain and family level modeling predicted at least two additional zinc finger domains in this
378 region (Fig. S10,Fig. S11). We also found many phosphorylated sites surrounding the zinc finger
379 domains. Examining mutations between *Anisota* and *Dryocampa* revealed three mutations mapped to
380 these predicted functional regions (Fig. 6B).
381 Given *disco's* adult diel-specific expression in moths, additional zinc-finger DNA binding
382 domains, and the high number of phosphorylated sites, we propose it as a candidate transcriptional
383 regulator for diel-regulation in adult moths.
384
385 ***Study species and their evolution and variation in life histories***
386 *Anisota* and *Dryocampa* are closely related and ecologically similar saturniids of the subfamily
387 Ceratocampinae, thought to have diverged ~3.81 Mya (47). They largely occupy the same range and
388 forest habitat in the Americas, feeding on large trees (*Anisota* on oaks and *Dryocampa* on maples)

where population flares cause host plant defoliation (38). Because they reportedly hybridize (94), and pre- and postzygotic barriers are potentially ineffective, temporal partitioning may be important in their evolutionary history.

Conclusion

This study provides a framework for how diel-niche evolution in Lepidoptera can occur. Sensory and neural developmental genes appear to be key. We identify the pivotal role of the transcription factor *disco*, uncovering a second functional region with species-specific mutations in moths. Our findings provide useful targets for further genetic manipulation and highlight the insight non-model systems provide to genetics and development.

Supplementary information

Supplementary tables and data are available for the reviewers and will be uploaded to repository [xxxxx] on submission.

.

Author contributions

Y.S.: conceptualization, data curation, formal analysis, investigation, methodology, project administration, software, visualization, writing–original draft. R.M: investigation, methodology, project administration, data curation, writing - review & editing. A.J.: conceptualization, formal analysis, writing - review & editing C.S.: conceptualization, data curation, methodology, project administration, supervision. S.C.: formal analysis, software. K.G.: formal analysis, software, visualization, writing-review and editing, D.G.: investigation, project administration, data curation. R.L.: conceptualization, data curation, investigation, methodology, writing-original draft, writing -review & editing. C.H.: conceptualization, data curation, investigation, methodology, project administration, writing - review and editing I.K.: conceptualization, funding acquisition, methodology, resources, writing–review and editing. C.E.: formal analysis, software, visualization, data curation, writing- original draft, writing- review & editing. C.B.: software, validation, writing -review and editing. S.B.: funding acquisition, methodology, validation, writing–review and editing. J.T: conceptualization, funding acquisition, supervision, validation, writing–review & editing. A.K: conceptualization, methodology, resources, writing–review and editing, visualization, supervision, funding acquisition

Acknowledgements

We thank Jesse Breinholt, Martijn Timmermans and Andreas Zwick for help with project conceptualization. Kelly Dexter, Amanda Markee, and members of the McGuire Center for Lepidoptera and Biodiversity at the University of Florida assisted with animal care and wet-lab troubleshooting. We thank Belinda Pinto, Danielle DeLeo, Heather Bracken-Grissom, Jorge Perez-Moreno, Zhou Lei for discussions, advice and assistance with bioinformatics pipelines and wet-lab protocols. We thank Nicolas Alexandre, Sachit Daniel, Riddhi Deshmukh, David Plotkin, Chelsea Skojec and Nitin Ravikanthachari for comments and feedback on the manuscript. Janelle Nunez-Castilla, Jessica Liberles, Raghavan Venket, Yi-Ming Weng, Yu Fahong and Xiaokang Zhang assisted with troubleshooting bioinformatic pipelines and provided analytical recommendations. The authors acknowledge the University of Florida Research Computing for providing computational resources and support that have contributed to the research results reported in this publication (http://researchcomputing.ufl.edu). We acknowledge NBAF and UF-ICBR for assistance with sequencing and generating libraries.

Funding for the project was through NSF DEB-1557007, NSF PRFB-1612862, and NSF IOS-1750833 and NERC NE/P003915/1. The Florida International University Presidential fellowship supported YS.

Figure Legends and Figures:

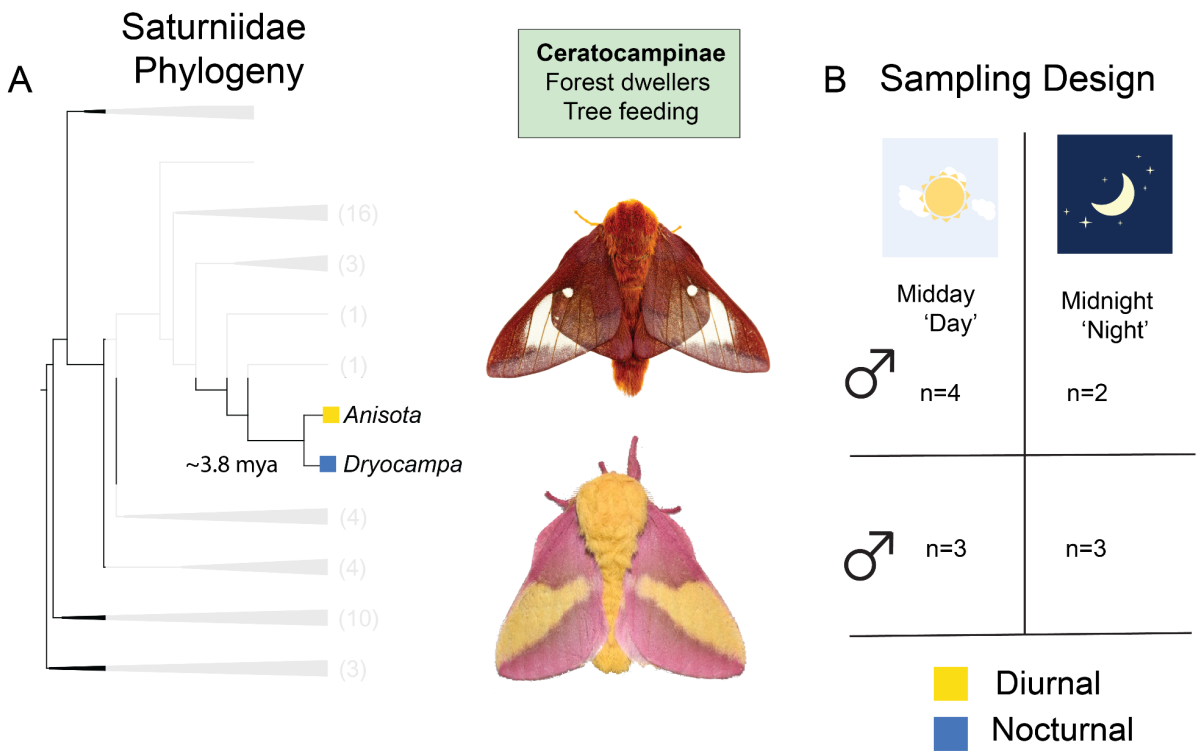

Figure 1: Nocturnal and diurnal moths on a phylogeny with RNA-seq sampling design.

(A): Collapsed phylogeny of Saturniidae, adapted to show where the two study species, diurnal *Anisota pellucida* (Pink-striped oakworm moth) and nocturnal *Dryocampa rubicunda* (Rosy Maple moth) sit. Faded numbers on the tip represent the number of genera in the tree before collapsing. Phylogeny adapted from Rougerie et al. 2022 (**B)**: Sampling design showing the number of replicates for each species and collection period (day/night) sampled. Collection of heads was done 2-days post eclosion at midday (sun) and midnight (moon) and tissue was flash frozen for RNA preservation. Care was taken that the eclosed moths were exposed to a natural light cycle and red lights were used when collecting the moths at night. Photo credits *Anisota pellucida* © Mike Chapman; *Dryocampa rubicunda* (CC) Andy Reacgo and Chrissy Mclearan;

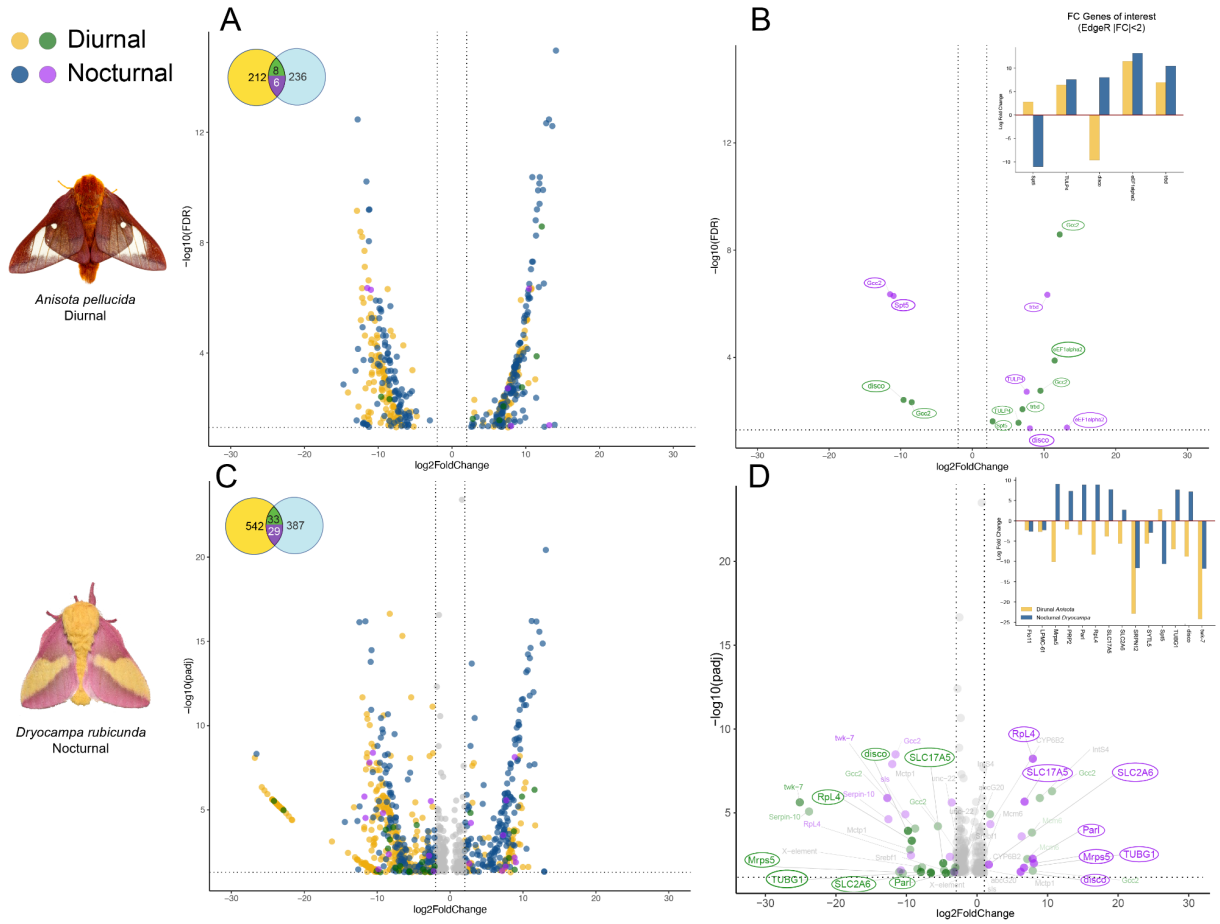

Figure 2: Nocturnal and diurnal species show divergent patterns of gene expression across two different analyses software (EdgeR and DESeq2)

Volcano plots and Venn diagrams showing EdgeR (A-B) and DESeq2 (C-D) results across **day vs. night** sampling times for both nocturnal and diurnal species. Venn diagrams represent the number of differentially expressed genes (DEGs) across both species with the number of common DEGs across each pair. **(A/C)**: Volcano diagrams illustrating fold change and adjusted p-values for the significant differentially expressed genes between midday and midnight samples. Circles in the top left represent the number of genes expressed in both species and the colors correspond to FC values for those genes in the volcano plots. Yellow and blue represent genes expressed only in the nocturnal or diurnal species, green/purple indicates DEGs present in both species. **(B/D)**: Only genes expressed in both species are shown and genes that display opposite trends in expression are highlighted. See Supplementary Material for a detailed list of DEGs. Positive fold change indicates night overexpression and negative fold change indicates day overexpression. Genes had FDR or adjusted p-value < 0.05 and FC > |2|. Identification of common genes was done using orthogroup clustering with Orthofinder with *Bombyx mori*. Gene names and annotations were transferred from *B. mori.*

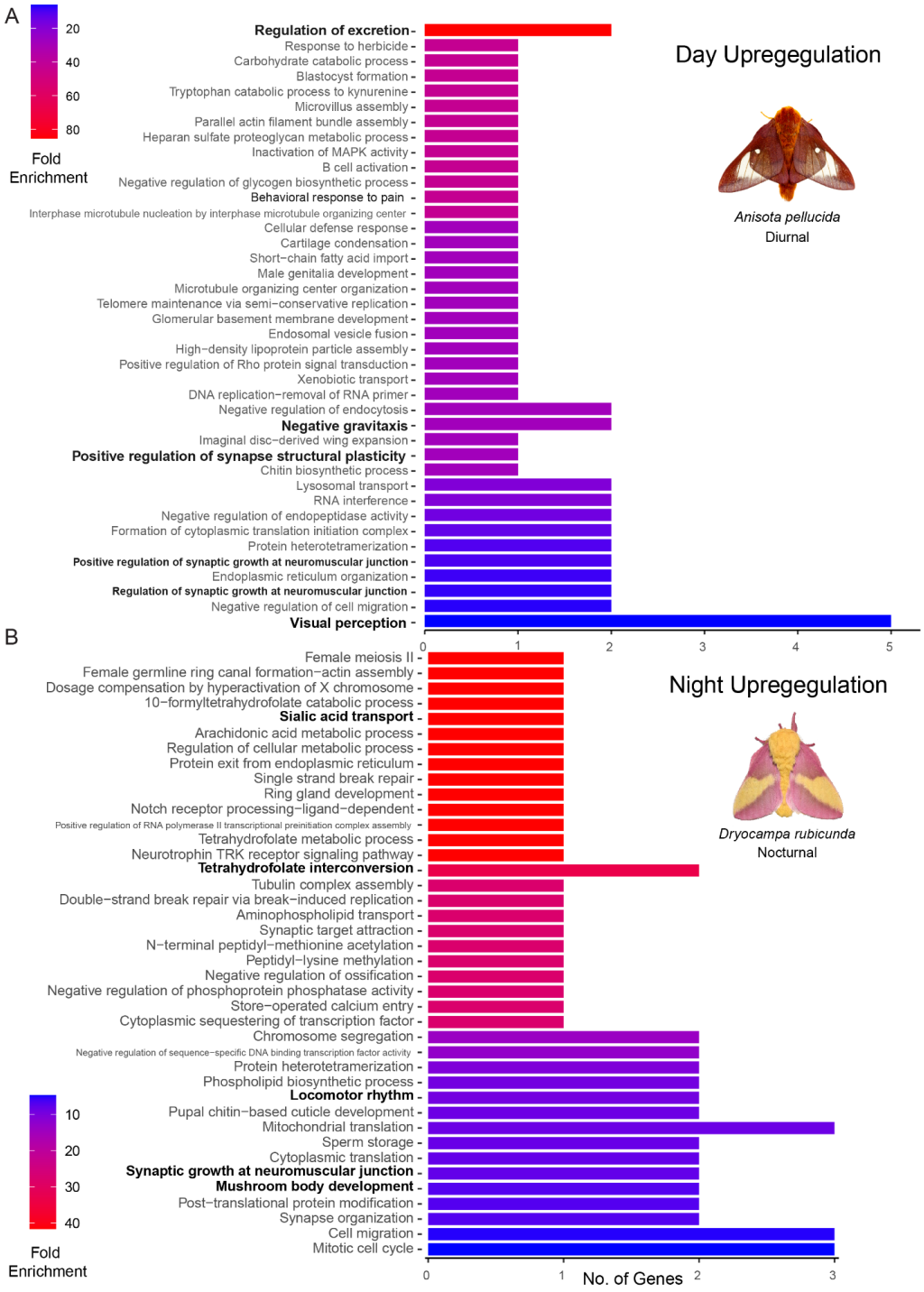
A
20
40
60
80
Fold Enrichment
Regulation of excretion
Response to herbicide
Carbohydrate catabolic process
Blastocyst formation
Tryptophan catabolic process to kynurenine
Microvillus assembly
Parallel actin filament bundle assembly
Heparan sulfate proteoglycan metabolic process
Inactivation of MAPK activity
B cell activation
Negative regulation of glycogen biosynthetic process
Behavioral response to pain
Interphase microtubule nucleation by interphase microtubule organizing center
Cellular defense response
Cartilage condensation
Short−chain fatty acid import
Male genitalia development
Microtubule organizing center organization
Telomere maintenance via semi−conservative replication
Glomerular basement membrane development
Endosomal vesicle fusion
High−density lipoprotein particle assembly
Positive regulation of Rho protein signal transduction
Xenobiotic transport
DNA replication−removal of RNA primer
Negative regulation of endocytosis
Negative gravitaxis
Imaginal disc−derived wing expansion
Positive regulation of synapse structural plasticity
Chitin biosynthetic process
Lysosomal transport
RNA interference
Negative regulation of endopeptidase activity
Formation of cytoplasmic translation initiation complex
Protein heterotetramerization
Positive regulation of synaptic growth at neuromuscular junction
Endoplasmic reticulum organization
Regulation of synaptic growth at neuromuscular junction
Negative regulation of cell migration
Visual perception
0
1
2
3
4
5
Day Upregegulation
Anisota pellucida
Diurnal
B
Female meiosis II
Female germline ring canal formation−actin assembly
Dosage compensation by hyperactivation of X chromosome
10−formyltetrahydrofolate catabolic process
Sialic acid transport
Arachidonic acid metabolic process
Regulation of cellular metabolic process
Protein exit from endoplasmic reticulum
Single strand break repair
Ring gland development
Notch receptor processing−ligand−dependent
Positive regulation of RNA polymerase II transcriptional preinitiation complex assembly
Tetrahydrofolate metabolic process
Neurotrophin TRK receptor signaling pathway
Tetrahydrofolate interconversion
Tubulin complex assembly
Double−strand break repair via break−induced replication
Aminophospholipid transport
Synaptic target attraction
N−terminal peptidyl−methionine acetylation
Peptidyl−lysine methylation
Negative regulation of ossification
Negative regulation of phosphoprotein phosphatase activity
Store−operated calcium entry
Cytoplasmic sequestering of transcription factor
Chromosome segregation
Negative regulation of sequence−specific DNA binding transcription factor activity
Protein heterotetramerization
Phospholipid biosynthetic process
Locomotor rhythm
Pupal chitin−based cuticle development
Mitochondrial translation
Sperm storage
Cytoplasmic translation
Synaptic growth at neuromuscular junction
Mushroom body development
Post−translational protein modification
Synapse organization
Cell migration
Mitotic cell cycle
Night Upregegulation
Dryocampa rubicunda
Nocturnal
10
20
30
40
Fold Enrichment
0
1
2
3
No. of Genes

Figure 3: Visual genes are upregulated in the diurnal species during the day, and energy utilization, brain olfactory region and locomotion in the nocturnal species during the night.
Go enrichment of highly upregulated genes recovered from both DEG analyses coinciding with the species. highlighting the two modules that showed species specific clustering patterns.
A: Enrichment of **day** upregulated genes in diurnal *Dryocampa*. B Enrichment of **night** upregulated genes in nocturnal *Anisota.* Go enrichment was done using the custom ShinyGo database v0.75c using *Bombyx* gene IDs. FDR cutoff <=0.17, and only Biological Process GO terms were selected with Min. pathway size =1. Input genes had FC>5, padj. <0.05 and recovered both in EdgeR and DeSeq2 were used with the background being all orthologous *Bombyx mori* genes for either species.

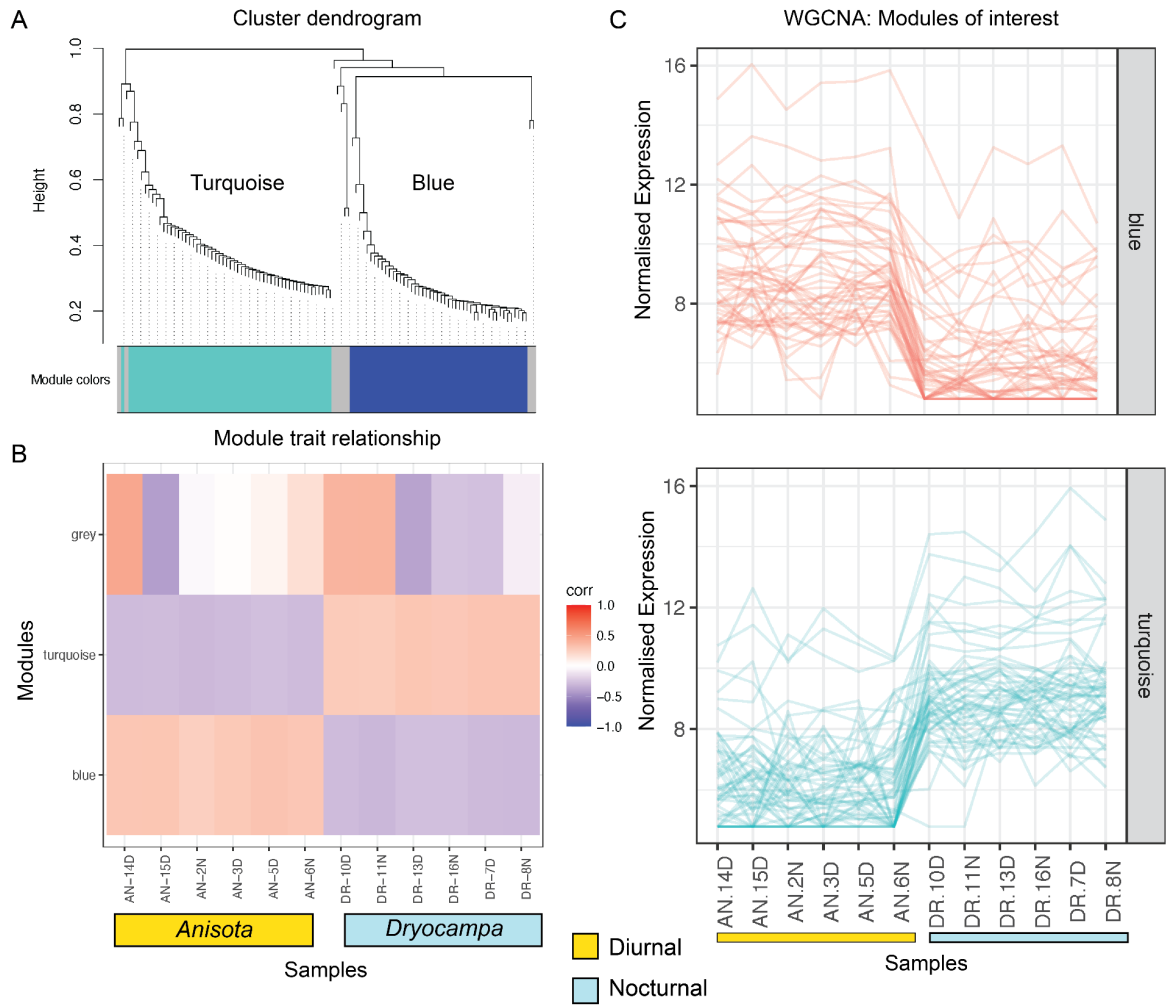

Figure 4: Modules of clustered co-expressed genes grouped using normalized expression highlighting the two modules that showed species specific clustering patterns.
A: Cluster dendrogram shows WGCNA clusters. B: Shows how patterns of gene expression correlate

486 across samples and modules. C: Shows the normalized expression for all
487 genes across samples. The species show two sets of 50 genes (Blue) and (Turquoise) that have clear
488 species specific expression patterns. Normalization was done with DESeq2 and reads were mapped
489 to the more stringently filtered transcriptome. A soft power analysis was done and the picked
490 power=9 for the WGCNA analysis. AN: *Anisota*, DR: *Dryocampa,* Numbered D and N represent the
491 different samples collected at day and night time points.

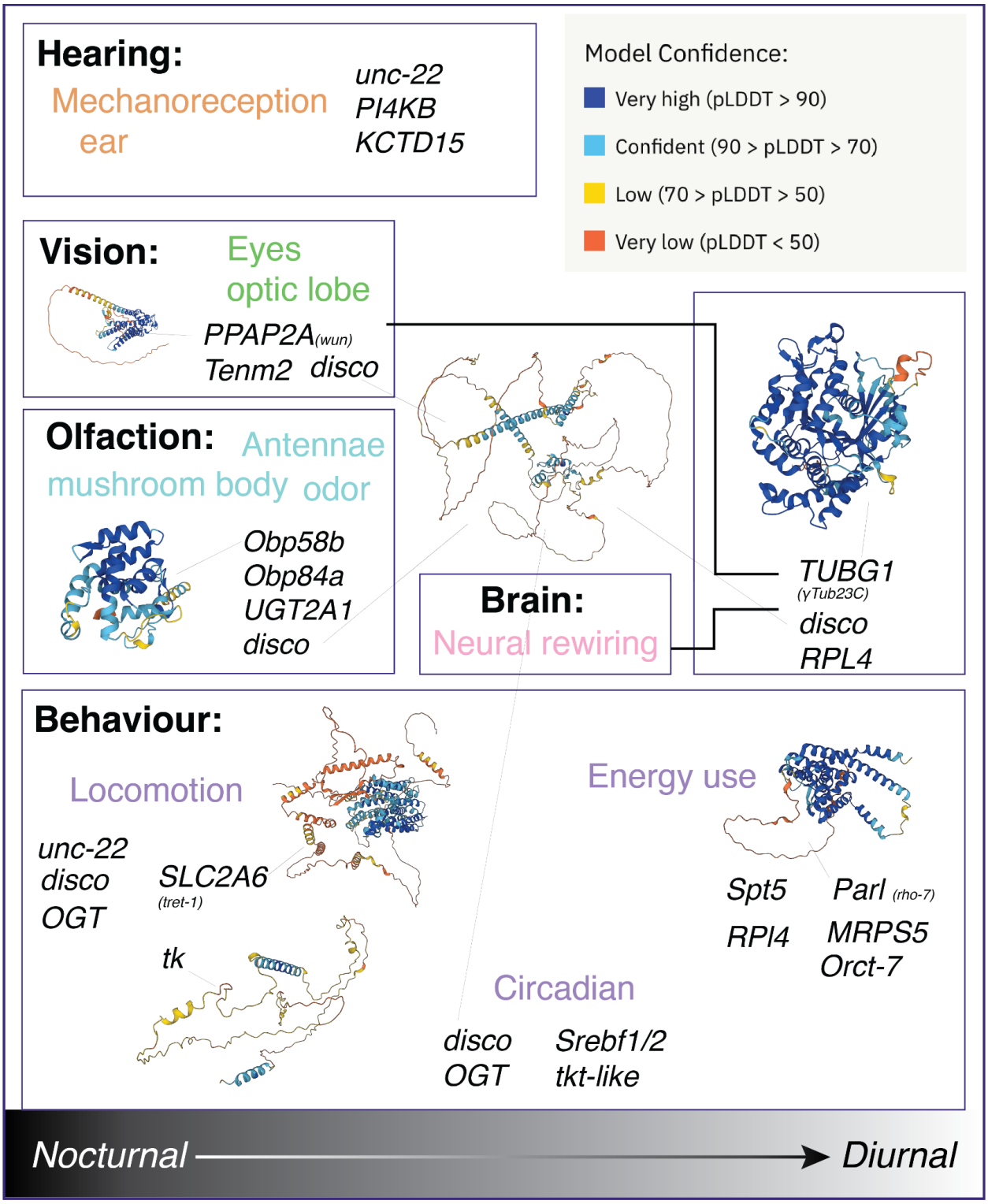

Figure 5: Model for diel-niche shift from and genes of interest obtained from GO searches and annotating divergently expressed genes. For representative purposes, homologs from *Drosophila*

melanogaster have been used, with colors in the 3d structures representing Alpha fold per-residue confidence metric (pLDDT), the range for each color is shown on the top left. Model moth *(Bombyx mori)* proteins were also modeled for a subset of proteins, see Supplementary data.

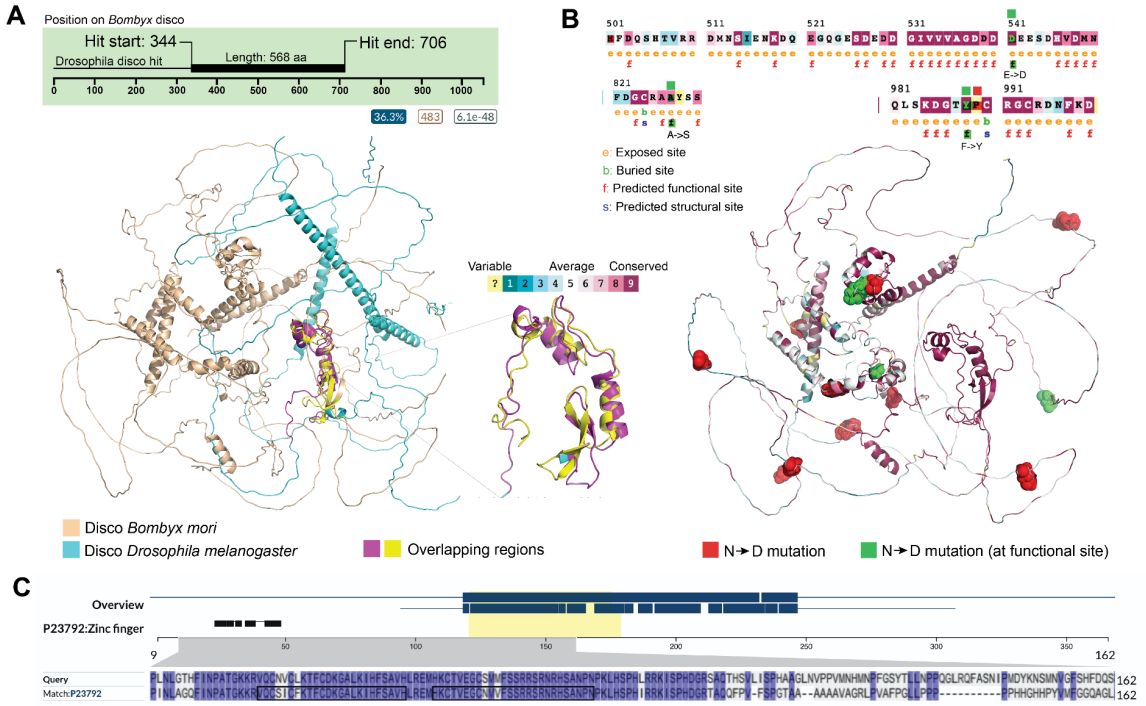

Figure 6: *Disco* has 150 amino acid long highly conserved region across *Bombyx* (1054 aa) & *Drosophila* (568 aa) involved in its role as a transcription factor, but it also has other roles in Lepidoptera due to the presence of other highly conserved and predicted functional regions, that are not present in flies, and only in Lepidoptera. 3/14 of the mutations between nocturnal to diurnal species map to these regions (>500 aa).
(A) Top: *Disco* best Uniprot hit in *Drosophila* using default settings (blastp, e-threshold 10, Auto-Blosum62). Bottom: *disco* aligned and superimposed predicted structures for the silk moth and vinegar fly. Peach structure: *Bombyx mori* alpha-fold predicted structure for *disco,* Cyan: *Drosophila melanogaster* alpha-fold predicted structure for *disco* **(B)** Top: Partial views of the Consurf predicted residues for *disco.* The views encompassing the region where 3 mutations of the 14 mutated sites between Nocturnal *Dryocampa* and Diurnal *Anisota* overlap with predicted functional residues. Bottom: Residues that were mutated between the nocturnal and diurnal species are highlighted on an overlay of the Consurf scores mapped onto the predicted alpha fold structure of disco from *Bombyx mori.* Green residues indicate mutated and predicted functional sites, red indicate mutated sites that did not have a predicted residue. **(C)** Overlap of the highly conserved region of *disco* this region includes the zinc-finger domain that is characteristic of disco transcription factor.

517

518 ## Supplemental Methods

519 **Insect rearing:**

520 Moths were reared under natural light-dark cycles at room temperature (25°C) and natural light
521 conditions at the McGuire Center for Lepidoptera and Biodiversity (MGCL). Adults were sampled
522 two days after eclosion at the two time points by C.H. and R.S.L.

523

524 **Sampling design:**

525 We collected 3-5 replicates (i.e., individual moths) per experimental treatment. We sampled at two
526 time points per species at two midpoints of their circadian cycle at noon ('day') and midnight
527 ('night') (Fig. 1, Table 1). Moths were allowed to eclose naturally and sexed, To ensure vision genes
528 were not artificially stimulated, for collection at night we used red light, which is thought to not
529 stimulate most Lepidoptera insect visual systems (95). We used a sterilized scalpel to remove the
530 head, which was placed in a 1.5 ml Eppendorf tube, which was immediately placed in liquid
531 nitrogen and stored at -80°C. It is worth noting that only males of most *Anisota* species are diurnal,
532 including *A. pellucida*, our focal taxon. Females of all *Anisota* and both sexes of at least *A. stigma*,
533 are nocturnal. In *Dryocampa*, both males and females are nocturnal. We therefore limited our
534 transcriptomic work to males of *A. pellucida* and *D. rubicunda*.

535

536 **RNA extraction and quality control:**

537 Tissue was removed from liquid nitrogen and placed into a flat-bottomed cryo-tube with Trizol and
538 2-4 sterile, stainless-steel beads. The tissue was homogenized using a bead beater for 2.5 minutes at
539 1900 RPM. Beads were removed with a magnet, and chloroform added to separate phases.
540 Isopropanol precipitated the RNA, followed by several ethanol wash steps to pellet the RNA. Quality
541 Control (QC) was undertaken with a high sensitivity Qubit assay. Samples with yields > 20 ng/µL
542 were cleaned using a Thermo Scientific RapidOut DNA Removal Kit (Waltham, Massachusetts,
543 USA). Sample quality was verified using Agilent 2200 Tapestation. Since heads comprised of a
544 relatively small amount of tissue, initial extractions using kit-based methods resulted in low yields.
545 Several rounds of troubleshooting were required before completion of extraction using a modified
546 Trizol based protocol with a DNA clean up step. We measured the quantity of RNA using a Qubit

547 fluorometer and used Agilent tapestation or Bioanalyzer to characterize extraction quality, weight,
548 and size distributions. Where possible, a concentration of more than 10 ng/µL was used for library
549 preparation. Yields below 10 ng/µL were prone to higher loss when purifying with a DNAse agent,
550 which often caused 20-30 % loss in RNA yield, approaching 5ng/µL is below the Qubit detection
551 threshold (Table S1).
552
553 **Library preparation and NGS sequencing:**
554 Libraries were prepared by sequencing cores at NBAF-Liverpool using the NEB polyA selection and
555 NEBNext Ultra II directional stranded kit, suitable for low input yields. 12 samples were run on one
556 lane of an Illumina NovaSeq using SP chemistry (Paired-end, 2x150 bp sequencing). Samples were
557 shipped overnight from MCGL to the NERC-NBAF after dehydrating in a biosafety chamber using
558 GenTegra RNA tubes.
559
560 **Read trimming and cleanup:**
561 For *Anisota pellucida* and *Dryocampa rubicunda*, trimming was undertaken by the NERC-NBAF
562 core and the raw Fastq files were trimmed for the presence of Illumina adapter sequences using
563 Cutadapt version 1.2 (96). The option -O 3 was used, so the 3' end of any reads that match the
564 adapter sequence for 3 bp or more were trimmed. Trimming was also done with trimmomatic. The
565 reads are further trimmed using Sickle version 1.200 with a minimum window quality score of 20.
566 Reads shorter than 15 bp after trimming were removed.
567
568 **Transcriptome library sizes, QC, and PCA:**
569 Quality Control (QC) was conducted on the trimmed reads, library size varied for each species (Fig.
570 S1). We examined expression data and removed genes with TPM < 1. PCA results showed that
571 *Anisota* and *Dryocampa* did not separate with diel-niche (Fig. S3).
572
573 ***De novo* assemblies:**
574 We combined reads from multiple samples and generated several reference de novo transcriptomes
575 using different assemblers, and then combining them, compared their quality using BUSCO scores
576 and number of single-copy BUSCO genes across the different versions (see Table 2 for the BUSCO

577 scores, redundancy and duplication for the various assemblies). We found that unfiltered assemblies
578 were highly redundant, but had the highest BUSCO scores. These assemblies were too
579 overrepresented to be used in any downstream analysis so we used Transrate, CD-HIT, MMeqs2, as
580 well as Transdecoder, to filter the assemblies. We chose v5 and v6 to use in downstream analysis,
581 listed as the last two assemblies for each species (Table 3) and repeated certain analyses with both
582 assemblies to see how stringent or a less stringent filter would affect the results.
583
584 **Multi assembler *de novo* transcriptome assembly:**
585 To our knowledge, there is no publicly available annotated reference genome for the two species
586 used in this study at the time the analyses were performed; therefore, we chose to build a de novo
587 transcriptome assembly with the pre-processed reads using the NCGAS pipeline, which combines
588 multiple assemblers and then uses an evidence-based gene modeler to decide on the final set. For
589 each species, we combined forward and reverse reads from all samples and normalized them using a
590 normalization script in Trinity v2.12.0 (97). Normalized reads were used as input to generate
591 assemblies using Velvet v1.2.10 (98), TransAbyss v2.0.1 (99) , SOAPdenovo v1.03 (100) with
592 various kmer sizes. These assemblies were combined and filtered using Evigenes v4: 2020, March
593 (101, 102), transdecoder and filtered with scripts provided in the NCGAS pipeline (103).
594
595 **Transcriptome QC, annotation and filtering:**
596 Further quality control and filtering was conducted using BUSCO (104), transrate (105), QUAST
597 (106) (v5.02), CD-HIT(v4.6.8) (107, 108)and cascaded clustering with MMseqs2 (v12) (109).
598 BUSCO scores were greater than 95%, but many genes had multiple versions from the different
599 assemblers, and because this would bias the downstream analyses we attempted to reduce the
600 redundancy at the cost of lowering BUSCO scores. Protein coding regions were predicted using
601 TransDecoder (https://github.com/TransDecoder/TransDecoder) and the cds file from was run
602 through Transrate (105), which further pulled contigs based on mapping rate and identified a "good"
603 collection of transcripts, the resulting protein-coding sequences were filtered with additional CD-HIT
604 (107, 108)and MMseqs2 (109) filtering. This resulted in lower BUSCO scores 75-85% but also much
605 lower redundancy in the gene set of about 1-3 fold. We ran the WGCNA (52) and GO enrichment
606 (110) analyses on the more stringent assemblies (BUSCO 75%, 2% genes with duplication) since

607 they are more sensitive to redundancy, but RNA-seq was run across the slightly lower stringency
608 analyses to be more inclusive (BUSCO~85%, 60-70% genes with duplications).
609
610 **Annotation of reference transcriptomes:**
611 Reference genomes were annotated with eggNOGmapper and Orthofinder (54, 55). We also tried
612 annotating the reference transcriptomes with Trinotate (111), which run against the swissprot and
613 pfam databases using hmmscan, blastx, blastp, signalP and tmmhmm, KEGG, and GO and eggNOG
614 (49, 110, 112–120). ORF predictions for orthofinder were obtained using *Antheraea pernyi* as a
615 model. Orthofinder was run with well-annotated Bombycidae and Saturniidae moths, *Bombyx mori*,
616 *Antheraea pernyi*, and *Antheraea yamamai*, to generate clusters. *Bombyx mori* was a useful reference
617 since the Orthofinder cluster for each species generated a list of mostly single-copy genes for which
618 more Lepidoptera annotations were available from SilkDBv3 (40). While this was not as complete as
619 trinotate, the annotations provided from this procedure were more accurate than Trinotate. Trinotate
620 annotation had many more human/ vertebrate hits than insect matches than eggNOGmapper and
621 Orthofinder transferred annotations, so while the files are provided as a reference, they were not used
622 in downstream analyses.
623
624 **Differential gene expression (DGE):**
625 Reads were mapped using Salmon (121) and differential gene expression analysis was conducted
626 using EdgeR (122) and DESeq2 (123). EdgeR(v 3.38.1) was used to normalize and test for
627 significantly expressed genes. DESeq2(v1.36.0) was also used to normalize and to generate PCAs
628 and other summary statistics. We used 'Day' as the treatment and 'Night' as the control for all
629 groups with EdgeR, although the order of fold change switched for DESeq2. The p-values obtained
630 were adjusted to account for multiple hypothesis testing with FDR for EdgeR and adjusted p-value
631 from DESeq2. Genes with FDR or adjusted p-values <0.05 and $|FC| > 2$ were used as a criteria to
632 identify significantly expressed genes.
633
634 **Gene enrichment analysis:**
635 We performed gene enrichment analysis using GO terms with the tools TopGO v2.48.0 (124) and
636 ShinyGo v0.75c (125) (http://bioinformatics.sdstate.edu/goc/). This analysis involved comparing the

637 selected genes of interest to a gene universe with GO term annotations to determine if there were
638 overrepresented or underrepresented GO terms. To obtain genes with GO annotations, we utilized
639 similarity clusters to map annotations from *Bombyx mori*.
640 In TopGO, we employed a more stringent approach by using filtered transcriptomes to
641 mitigate bias from gene duplications. We selected genes of interest based on a False Discovery Rate
642 (FDR) threshold of less than 0.05. We ran two different enrichment algorithms, 'classic' and 'elim',
643 and used two test statistics, Fisher's exact test and a Kolmogorov-Smirnov-like test. The tests were
644 performed for both 'Biological Process' (BP) and 'Molecular Function' (MF) categories. While we
645 generated tables of significantly enriched GO terms, obtaining individual genes within each group
646 was limited due to the constraints of TopGO with custom annotations.
647 For ShinyGO, we utilized the custom v0.75c which included the updated *Bombyx mori*
648 genome stringent. For all analysis, we used the following settings (pathway size: min.=1,
649 max=2000). The settings for number of pathways to show and FDR cut-offs were chosen to represent
650 the entire list of top 100 genes in the final datasets, although in some cases a fewer number are
651 represented in the visualizations. We focused on the 'Biological Process' (BP) category for the
652 various tests. Tables of GO terms, gene information, and graphs summarizing the significantly
653 enriched GO terms were generated. We repeated several different analyses **1)** A less stringent
654 analysis was run where genes with FC<|2| and padj. <0.05. This was useful to visualize the genes up
655 and downregulated functionally and the background used was all the genes recovered from the DEA
656 analysis that had orthologs. An FDR cut-off <0.1-0.3. For the background gene set, we used the
657 species' de-novo transcriptome matching *Bombyx* ortholog set.
658 **2)** A more stringent criteria was used to examine highly upregulated genes a FC<|5| and padj.
659 <0.05 cutoff was used, and filtering only genes that occurred in both EdgeR and DESeq2 analyses.
660 We selected a single representative when multiple Bombyx orthologs were recovered, using the
661 ortholog with the most complete annotation. An FDR cut-off <0.17 was used. For the background
662 gene set, we used the species' de-novo transcriptome matching Bombyx ortholog set.
663 **3)** For WGCNA clusters tan and grey60, we used their respective species background
664 expressed transcript set with a FDR cutoff <= 0.1. For blue and turquoise, the background of all
665 orthologs found in *Bombyx mori* was used. An FDR cutoff<1 was used, since smaller values
666 provided insufficient genes given the larger number of genes being tested.

667

668 **Gene network analysis:**

669 Gene network analysis was undertaken with WGCNA (1.71) (52, 126). DeESeq2 was used to
670 normalize reads and data was formatted with tidyverse. WGCNA identifies modules of co-expressed
671 genes. We chose modules that showed clear day-night differences and mapped the GO terms with
672 Revigo and ShinyGo. We also combined counts from both species and tested for clusters. Here we
673 chose modules that showed species specific clusters.

674

675 **Gene annotation and filtering:**

676 DEGs, enriched genes and or co-expressed transcripts/ genes were annotated by cross referencing
677 them with the *B. mori* annotations (see above). Since *B. mori* mappings were not always 'one-to-
678 one', mappings that were 'one-to-many' were dropped, i.e., transcripts that mapped to multiple
679 *Bombyx* genes were dropped. We also improved annotation by mapping the overlapping transcripts
680 with eggnog mapper. We further filtered these genes into sub functional categories, by identifying
681 genes with GO annotations or descriptions linked to vision, smell, hearing, circadian, behavior and
682 brain the list of go terms for each group was obtained by querying amigo
683 (http://amigo.geneontology.org/) (Table 8).

684

685 **Gene Mining and in-silico evolution:**

686 We mined genes of interest from ~bombycoidea moths and closely related families that had well
687 annotated genomes on Ensembl and NCBI (Supp Table 6) and across model insects (Supp. Table 7).
688 These genomes were chosen as all Bombycoidea from Ensembl with well annotated assemblies and
689 five species Noctuidae and Geometridae each were included as close relatives. We added *Bombyx*
690 *mori* as a reference and *Antheraea pernyi* to represent Saturniidae, and their peptide files were taken
691 from their respective source papers (40–42). For insects, we chose long-read well annotated genomes
692 from Ensembl (Ensembl Gene build) and five model systems from insect base (127). We ran
693 Orthofinder (v2.5.2) (49, 55) with 'orthofinder -f bom-rel/ -S diamond -M msa -A mafft -T fasttree -a
694 1 -X -z -t 16' to recover orthologs. Each orthogroup often contained multiple sequences per species.
695 We chose the sequence with the highest identity to the reference *Bombyx mori* sequence using
696 custom python scripts. In the rare instances where there were multiple references, we took the longest

one. To model the 3D structure of each reference *Bombyx mori* sequence, we ran AlphaFold v2.1.2 (128) using Deepmind's run_alphafold.py (https://github.com/deepmind/alphafold/blob/main/run_alphafold.py) on University of Florida's HiperGator. Model database files (i.e. BFD, MAGnify, PDB70, mmCIF PDB, UniRef30, UniRef90) downloaded from Deepmind in February 2022 were used as parameter value inputs. All other parameters were used with default settings. The relaxed predicted model with highest ranked pLDDT (per-residue estimate corresponding to model's predicted score on the lDDT-Cα metric) was chosen as the final model (129).

We calculated a conservation score for each alignment using Alistat. For alignments less than 1500 amino acids and with high conservation score (Proteins larger than 1300 aa were difficult to model without high memory GPU's), we modeled conservation using Consurf (130–134). The results were displayed using Jmol first glance viewer (http://firstglance.jmol.org/) and as screenshots from the default viewer. The output for alpha fold runs and consurf is available in the (Supplementary Data). PyMol (135) was used to align the 3D structures and Aliview was used to compare alignments. We used InterProscan (https://www.ebi.ac.uk/interpro/about/interproscan/) and NetPhos3.1 (136, 137) for predicting the domains and phosphorylated sites.

References

1. Y. Xiao, Y. Yuan, M. Jimenez, N. Soni, S. Yadlapalli, Clock proteins regulate spatiotemporal organization of clock genes to control circadian rhythms. *Proc. Natl. Acad. Sci. U. S. A.* **118** (2021).

2. K. Beer, C. Helfrich-Förster, Model and Non-model Insects in Chronobiology. *Front. Behav. Neurosci.* **14**, 601676 (2020).

3. D. Székely, D. Cogălniceanu, P. Székely, M. Denoël, Adult-Juvenile interactions and temporal niche partitioning between life-stages in a tropical amphibian. *PLoS One* **15**, e0238949 (2020).

4. D. Wang, G. Yang, W. Chen, Diel and Circadian Patterns of Locomotor Activity in the Adults of Diamondback Moth (Plutella xylostella). *Insects* **12** (2021).

5. J. H. Fullard, N. Napoleone, Diel flight periodicity and the evolution of auditory defences in the Macrolepidoptera. *Anim. Behav.* **62**, 349–368 (2001).

6. R. Refinetti, The diversity of temporal niches in mammals. *Biol. Rhythm Res.* **39**, 173–192 (2008).

7. A. Y. Kawahara, *et al.*, Diel behavior in moths and butterflies: a synthesis of data illuminates the evolution of temporal activity. *Organisms Diversity and Evolution* **18**, 13–27 (2018).

8. D. T. C. Cox, A. S. Gardner, K. J. Gaston, Diel niche variation in mammals associated with expanded trait space. *Nat. Commun.* **12**, 1753 (2021).

9. Y. Basset, N. D. Springate, Diel activity of arboreal arthropods associated with a rainforest tree. *J. Nat. Hist.* **26**, 947–952 (1992).

10. P. J. Devries, G. T. Austin, N. H. Martin, Diel activity and reproductive isolation in a diverse assemblage of Neotropical skippers (Lepidoptera: Hesperiidae). *Biol. J. Linn. Soc. Lond.* **94**, 723–736 (2008).

11. S. R. Anderson, J. J. Wiens, Out of the dark: 350 million years of conservatism and evolution in diel activity patterns in vertebrates. *Evolution* **71**, 1944–1959 (2017).

12. S. Frey, J. T. Fisher, A. C. Burton, J. P. Volpe, Investigating animal activity patterns and temporal niche partitioning using camera-trap data: challenges and opportunities. *Remote Sens. Ecol. Conserv.* **3**, 123–132 (2017).

13. R. Steen, Diel activity, frequency and visit duration of pollinators in focal plants: in situ automatic camera monitoring and data processing. *Methods Ecol. Evol.* **8**, 203–213 (2017).

14. H. K. Gill, G. Goyal, R. McSorley, Diel Activity of Fauna in Different Habitats Sampled at the Autumnal Equinox. *Fla. Entomol.* **95**, 319–325 (2012).

15. B. Murugavel, A. Kelber, H. Somanathan, Light, flight and the night: effect of ambient light and moon phase on flight activity of pteropodid bats. *J. Comp. Physiol. A Neuroethol. Sens. Neural Behav. Physiol.* **207**, 59–68 (2021).

16. H. Somanathan, *et al.*, Nocturnal bees feed on diurnal leftovers and pay the price of day – night lifestyle transition. *Front. Ecol. Evol.* **8** (2020).

17. R. M. Borges, H. Somanathan, A. Kelber, Patterns and Processes in Nocturnal and Crepuscular Pollination Services. *Q. Rev. Biol.* **91**, 389–418 (2016).

18. S. M. Tierney, *et al.*, Consequences of evolutionary transitions in changing photic environments. *Austral Entomology* **56**, 23–46 (2017).

19. W. T. Wcislo, *et al.*, The evolution of nocturnal behaviour in sweat bees, Megalopta genalis and M. ecuadoria (Hymenoptera: Halictidae): an escape from competitors and enemies? *Biol. J. Linn. Soc. Lond.* **83**, 377–387 (2004).

20. A. L. Stockl, W. A. Ribi, E. J. Warrant, Adaptations for Nocturnal and Diurnal Vision in the Hawkmoth Lamina. *J. Comp. Neurol.* **524**, 160–175 (2016).

21. Y. Wu, *et al.*, Retinal transcriptome sequencing sheds light on the adaptation to nocturnal and diurnal lifestyles in raptors. *Sci. Rep.* **6**, 1–12 (2016).

22. T. Akiyama, H. Uchiyama, S. Yajima, K. Arikawa, Y. Terai, Parallel evolution of opsin visual pigments in hawkmoths by tuning of spectral sensitivities during transition from a nocturnal to a diurnal ecology. *J. Exp. Biol.* **225**, jeb244541 (2022).

763 23. Y. Sondhi, E. Elis, S. Bybee, J. Theobald, A. Kawahara, Light environment drives evolution of color
764 vision genes in butterflies and moths (2021) https:/doi.org/10.5061/dryad.gmsbcc2kr (May 13,
765 2022).

766 24. M. Izutsu, A. Toyoda, A. Fujiyama, K. Agata, N. Fuse, Dynamics of Dark-Fly Genome Under
767 Environmental Selections. *G3* **6**, 365–376 (2015).

768 25. J. E. Yack, J. H. Fullard, Ultrasonic hearing in nocturnal butterflies. *Nature* **403**, 265–266 (2000).

769 26. F. Sandrelli, R. Costa, C. P. Kyriacou, E. Rosato, Comparative analysis of circadian clock genes in
770 insects. *Insect Mol. Biol.* **17**, 447–463 (2008).

771 27. R. Závodská, I. Sauman, F. Sehnal, Distribution of PER protein, pigment-dispersing hormone,
772 prothoracicotropic hormone, and eclosion hormone in the cephalic nervous system of insects. *J. Biol.*
773 *Rhythms* **18**, 106–122 (2003).

774 28. C. Hermann, *et al.*, The circadian clock network in the brain of different Drosophila species. *J.*
775 *Comp. Neurol.* **521**, 367–388 (2013).

776 29. C. A. Hamilton, *et al.*, Phylogenomics resolves major relationships and reveals significant
777 diversification rate shifts in the evolution of silk moths and relatives. *BMC Evol. Biol.* (2019)
778 https:/doi.org/10.1186/s12862-019-1505-1.

779 30. A. Kobelková, R. Závodská, I. Sauman, O. Bazalová, D. Dolezel, Expression of clock genes period
780 and timeless in the central nervous system of the Mediterranean flour moth, Ephestia kuehniella. *J.*
781 *Biol. Rhythms* **30**, 104–116 (2015).

782 31. D. Brady, A. Saviane, S. Cappellozza, F. Sandrelli, The Circadian Clock in Lepidoptera. *Front.*
783 *Physiol.* **12**, 776826 (2021).

784 32. S. Iwai, Y. Fukui, Y. Fujiwara, M. Takeda, Structure and expressions of two circadian clock genes,
785 period and timeless in the commercial silkmoth, Bombyx mori. *J. Insect Physiol.* **52**, 625–637
786 (2006).

787 33. A. Macias-Muñoz, A. G. Rangel Olguin, A. D. Briscoe, Evolution of Phototransduction Genes in
788 Lepidoptera. *Genome Biol. Evol.* **11**, 2107–2124 (2019).

789 34. X.-C. Jiang, *et al.*, Identification of Olfactory Genes From the Greater Wax Moth by Antennal
790 Transcriptome Analysis. *Front. Physiol.* **12**, 663040 (2021).

791 35. A. de Fouchier, *et al.*, Functional evolution of Lepidoptera olfactory receptors revealed by
792 deorphanization of a moth repertoire. *Nat. Commun.* **8**, 15709 (2017).

793 36. J. W. Truman, L. M. Riddiford, Neuroendocrine control of ecdysis in silkmoths. *Science* **167**, 1624–
794 1626 (1970).

795 37. I. Sauman, S. M. Reppert, Circadian clock neurons in the silkmoth Antheraea pernyi: novel
796 mechanisms of Period protein regulation. *Neuron* **17**, 889–900 (1996).

797 38. P. M. Tuskes, J. P. Tuttle, M. M. Collins, *The Wild Silk Moths of North America: A Natural History*
798 *of the Saturniidae of the United States and Canada* (Cornell University Press, 1996).

799 39. M. M. Collins, P. M. Tuskes, REPRODUCTIVE ISOLATION IN SYMPATRIC SPECIES OF
800 DAYFLYING MOTHS (HEMILEUCA: SATURNIIDAE). *Evolution* **33**, 728–733 (1979).

801 40. F. Lu, *et al.*, SilkDB 3.0: visualizing and exploring multiple levels of data for silkworm. *Nucleic*
802 *Acids Res.* **48**, D749–D755 (2020).

803 41. S.-R. Kim, *et al.*, Genome sequence of the Japanese oak silk moth, Antheraea yamamai: the first
804 draft genome in the family Saturniidae. *Gigascience* **7**, 1–11 (2018).

805 42. J. Duan, *et al.*, A chromosome-scale genome assembly of Antheraea pernyi (Saturniidae,
806 Lepidoptera). *Mol. Ecol. Resour.* **20**, 1372–1383 (2020).

807 43. H. Langer, G. Schmeinck, F. Anton-Erxleben, Identification and localization of visual pigments in
808 the retina of the moth, Antheraea polyphemus (Insecta, Saturniidae). *Cell Tissue Res.* **245**, 81–89
809 (1986).

810 44. I. Kitching, *et al.*, A global checklist of the Bombycoidea (Insecta: Lepidoptera). *Biodiversity Data*
811 *Journal* **6**, e22236 (2018).

812 45. M. J. Scoble, *The Lepidoptera. Form, function and diversity* (Oxford University Press, 1992).

813 46. Lemaire, Minet, 18. The Bombycoidea and their Relatives. *Volume 1: Evolution, Systematics, and*
814 (2013).

815 47. R. Rougerie, *et al.*, Phylogenomics Illuminates the Evolutionary History of Wild Silkmoths in Space
816 and Time (Lepidoptera: Saturniidae). *bioRxiv*, 2022.03.29.486224 (2022).

817 48. Z. Wang, M. Gerstein, M. Snyder, RNA-Seq: a revolutionary tool for transcriptomics. *Nat. Rev.*
818 *Genet.* **10**, 57–63 (2009).

819 49. D. M. Emms, S. Kelly, OrthoFinder: solving fundamental biases in whole genome comparisons
820 dramatically improves orthogroup inference accuracy. *Genome Biol.* **16**, 157 (2015).

821 50. D. Li, *et al.*, An evaluation of RNA-seq differential analysis methods. *PLoS One* **17**, e0264246
822 (2022).

823 51. N. Sánchez-Baizán, L. Ribas, F. Piferrer, Improved biomarker discovery through a plot twist in
824 transcriptomic data analysis. *BMC Biol.* **20**, 208 (2022).

825 52. P. Langfelder, S. Horvath, WGCNA: an R package for weighted correlation network analysis. *BMC*
826 *Bioinformatics* **9**, 559 (2008).

827 53. Lafayette Lafayette Press, *A Survey of Best Practices for RNA-Seq Data Analysis* (CreateSpace
828 Independent Publishing Platform, 2016).

829 54. C. P. Cantalapiedra, A. Hernández-Plaza, I. Letunic, P. Bork, J. Huerta-Cepas, eggNOG-mapper v2:

Functional Annotation, Orthology Assignments, and Domain Prediction at the Metagenomic Scale. *Mol. Biol. Evol.* **38**, 5825–5829 (2021).

55. D. M. Emms, S. Kelly, OrthoFinder: phylogenetic orthology inference for comparative genomics. *Genome Biol.* **20**, 238 (2019).

56. P. E. Hardin, J. C. Hall, M. Rosbash, Behavioral and molecular analyses suggest that circadian output is disrupted by disconnected mutants in D. melanogaster. *EMBO J.* **11**, 1–6 (1992).

57. M. S. Dushay, M. Rosbash, J. C. Hall, The disconnected visual system mutations in Drosophila melanogaster drastically disrupt circadian rhythms. *J. Biol. Rhythms* **4**, 1–27 (1989).

58. K. J. Lee, M. Mukhopadhyay, P. Pelka, A. R. Campos, H. Steller, Autoregulation of the Drosophila disconnected gene in the developing visual system. *Dev. Biol.* **214**, 385–398 (1999).

59. V. Suri, Z. Qian, J. C. Hall, M. Rosbash, Evidence that the TIM light response is relevant to light-induced phase shifts in Drosophila melanogaster. *Neuron* **21**, 225–234 (1998).

60. B. K. Dey, X.-L. Zhao, E. Popo-Ola, A. R. Campos, Mutual regulation of the Drosophila disconnected (disco) and Distal-less (Dll) genes contributes to proximal-distal patterning of antenna and leg. *Cell Tissue Res.* **338**, 227–240 (2009).

61. H. Somanathan, A. Kelber, R. M. Borges, R. Wallén, E. J. Warrant, Visual ecology of Indian carpenter bees II: adaptations of eyes and ocelli to nocturnal and diurnal lifestyles. *J. Comp. Physiol. A Neuroethol. Sens. Neural Behav. Physiol.* **195**, 571–583 (2009).

62. A. L. Stöckl, D. O'Carroll, E. J. Warrant, Higher-order neural processing tunes motion neurons to visual ecology in three species of hawkmoths. *Proceedings of the Royal Society B: Biological Sciences* **284**, 20170880 (2017).

63. I. Shimizu, Y. Yamakawa, Y. Shimazaki, T. Iwasa, Molecular cloning of Bombyx cerebral opsin (Boceropsin) and cellular localization of its expression in the silkworm brain. *Biochem. Biophys. Res. Commun.* **287**, 27–34 (2001).

64. K. Moses, M. C. Ellis, G. M. Rubin, The glass gene encodes a zinc-finger protein required by Drosophila photoreceptor cells. *Nature* **340**, 531–536 (1989).

65. R. Tearle, Tissue specific effects of ommochrome pathway mutations in Drosophila melanogaster. *Genet. Res.* **57**, 257–266 (1991).

66. H. K. Shamloula, *et al.*, rugose (rg), a Drosophila A kinase anchor protein, is required for retinal pattern formation and interacts genetically with multiple signaling pathways. *Genetics* **161**, 693–710 (2002).

67. A. Stöckl, *et al.*, Differential investment in visual and olfactory brain areas reflects behavioural choices in hawk moths. *Sci. Rep.* **6** (2016).

68. A. Sourakov, R. W. Chadd, *The Lives of Moths: A Natural History of Our Planet's Moth Life* (Princeton University Press, 2022).

69. A. Y. Kawahara, *et al.*, Phylogenomics reveals the evolutionary timing and pattern of butterflies and moths. *Proc. Natl. Acad. Sci. U. S. A.* **116**, 22657–22663 (2019).

70. J. J. Rubin, *et al.*, The evolution of anti-bat sensory illusions in moths. *Science Advances* (2018) https:/doi.org/10.1126/sciadv.aar7428.

71. J. E. Yack, L. D. Otero, J. W. Dawson, A. Surlykke, J. H. Fullard, Sound production and hearing in the blue cracker butterfly Hamadryas feronia (Lepidoptera, nymphalidae) from Venezuela. *J. Exp. Biol.* **203**, 3689–3702 (2000).

72. J. R. Barber, *et al.*, Anti-bat ultrasound production in moths is globally and phylogenetically widespread. *Proc. Natl. Acad. Sci. U. S. A.* **119**, e2117485119 (2022).

73. G. A. Jacobs, J. P. Miller, Z. Aldworth, Computational mechanisms of mechanosensory processing in the cricket. *J. Exp. Biol.* **211**, 1819–1828 (2008).

74. J. M. Camhi, Locust wind receptors: I. Transducer mechanics and sensory response. *J. Exp. Biol.* **50**, 335–348 (1969).

75. J. M. Camhi, Locust wind receptors. 3. Contribution to flight initiation and lift control. *J. Exp. Biol.* **50**, 363–373 (1969).

76. J. C. Tuthill, R. I. Wilson, Mechanosensation and Adaptive Motor Control in Insects. *Curr. Biol.* **26**, R1022–R1038 (2016).

77. J. D. Baker, S. Adhikarakunnathu, M. J. Kernan, Mechanosensory-defective, male-sterile unc mutants identify a novel basal body protein required for ciliogenesis in Drosophila. *Development* **131**, 3411–3422 (2004).

78. D. D. Dell'Aglio, W. O. McMillan, S. H. Montgomery, Shifting balances in the weighting of sensory modalities are predicted by divergence in brain morphology in incipient species of Heliconius butterflies. *Anim. Behav.* **185**, 83–90 (2022).

79. S. H. Montgomery, R. M. Merrill, S. R. Ott, Brain composition in Heliconius butterflies, posteclosion growth and experience-dependent neuropil plasticity. *J. Comp. Neurol.* **524**, 1747–1769 (2016).

80. S. Anton, W. Rössler, Plasticity and modulation of olfactory circuits in insects. *Cell Tissue Res.* **383**, 149–164 (2021).

81. S. Halali, *et al.*, Predictability of temporal variation in climate and the evolution of seasonal polyphenism in tropical butterfly communities. *J. Evol. Biol.* **34**, 1362–1375 (2021).

82. W. Kuenzinger, *et al.*, Innate colour preferences of a hawkmoth depend on visual context. *Biol. Lett.* **15**, 20180886 (2019).

83. A. Kelber, Pattern discrimination in a hawkmoth: innate preferences, learning performance and ecology. *Proc. Biol. Sci.* **269**, 2573–2577 (2002).

899 84. G. T. Broadhead, T. Basu, M. von Arx, R. A. Raguso, Diel rhythms and sex differences in the
900 locomotor activity of hawkmoths. *J. Exp. Biol.* **220**, 1472–1480 (2017).

901 85. M. Bischoff, R. A. Raguso, A. Jürgens, D. R. Campbell, Context-dependent reproductive isolation
902 mediated by floral scent and color. *Evolution* **69**, 1–13 (2015).

903 86. S. Jaeger, C. Girvin, N. Demarest, E. LoPresti, Secondary pollinators contribute to reproductive
904 success of a pink-flowered sand verbena population. *Ecology* **104**, e3977 (2023).

905 87. W. V. So, *et al.*, takeout, a novel Drosophila gene under circadian clock transcriptional regulation.
906 *Mol. Cell. Biol.* **20**, 6935–6944 (2000).

907 88. T. Kikawada, *et al.*, Trehalose transporter 1, a facilitated and high-capacity trehalose transporter,
908 allows exogenous trehalose uptake into cells. *Proc. Natl. Acad. Sci. U. S. A.* **104**, 11585–11590
909 (2007).

910 89. H. Steller, K. F. Fischbach, G. M. Rubin, Disconnected: a locus required for neuronal pathway
911 formation in the visual system of Drosophila. *Cell* **50**, 1139–1153 (1987).

912 90. C. Helfrich-Förster, Robust circadian rhythmicity of Drosophila melanogaster requires the presence
913 of lateral neurons: a brain-behavioral study of disconnected mutants. *J. Comp. Physiol. A* **182**, 435–
914 453 (1998).

915 91. L. R. Sanders, M. Patel, J. W. Mahaffey, The Drosophila gap gene giant has an anterior segment
916 identity function mediated through disconnected and teashirt. *Genetics* **179**, 441–453 (2008).

917 92. E. Blanchardon, *et al.*, Defining the role of Drosophila lateral neurons in the control of circadian
918 rhythms in motor activity and eclosion by targeted genetic ablation and PERIOD protein
919 overexpression. *Eur. J. Neurosci.* **13**, 871–888 (2001).

920 93. A. D. Keller, T. Maniatis, Only two of the five zinc fingers of the eukaryotic transcriptional
921 repressor PRDI-BF1 are required for sequence-specific DNA binding. *Mol. Cell. Biol.* **12**, 1940–
922 1949 (1992).

923 94. S. Johnson, N. Boob, A strange pair. *News of the Lepidopterists' Society* **55**, 116 (2013).

924 95. C. J. van der Kooi, D. G. Stavenga, K. Arikawa, G. Belušič, A. Kelber, Evolution of Insect Color
925 Vision: From Spectral Sensitivity to Visual Ecology. *Annu. Rev. Entomol.* **66**, 435–461 (2021).

926 96. M. Martin, Cutadapt removes adapter sequences from high-throughput sequencing reads.
927 *EMBnet.journal* **17**, 10–12 (2011).

928 97. M. G. Grabherr, *et al.*, Full-length transcriptome assembly from RNA-Seq data without a reference
929 genome. *Nat. Biotechnol.* **29**, 644–652 (2011).

930 98. D. R. Zerbino, E. Birney, Velvet: algorithms for de novo short read assembly using de Bruijn graphs.
931 *Genome Res.* **18**, 821–829 (2008).

932 99. G. Robertson, *et al.*, De novo assembly and analysis of RNA-seq data. *Nat. Methods* **7**, 909–912

933 (2010).

934 100. R. Luo, *et al.*, SOAPdenovo2: an empirically improved memory-efficient short-read de novo
935 assembler. *Gigascience* **1**, 18 (2012).

936 101. D. G. Gilbert, Longest protein, longest transcript or most expression, for accurate gene
937 reconstruction of transcriptomes? *bioRxiv*, 829184 (2019).

938 102. D. Gilbert, Gene-omes built from mRNA seq not genome DNA (2016)
939 https:/doi.org/10.7490/f1000research.1112594.1 (June 6, 2022).

940 103. , *https://github.com/NCGAS/de-novo-transcriptome-assembly-pipeline* (Github) (June 6, 2022).

941 104. M. Manni, M. R. Berkeley, M. Seppey, F. A. Simão, E. M. Zdobnov, BUSCO Update: Novel and
942 Streamlined Workflows along with Broader and Deeper Phylogenetic Coverage for Scoring of
943 Eukaryotic, Prokaryotic, and Viral Genomes. *Mol. Biol. Evol.* **38**, 4647–4654 (2021).

944 105. R. Smith-Unna, C. Boursnell, R. Patro, J. M. Hibberd, S. Kelly, TransRate: reference-free quality
945 assessment of de novo transcriptome assemblies. *Genome Res.* **26**, 1134–1144 (2016).

946 106. A. Mikheenko, A. Prjibelski, V. Saveliev, D. Antipov, A. Gurevich, Versatile genome assembly
947 evaluation with QUAST-LG. *Bioinformatics* **34**, i142–i150 (2018).

948 107. W. Li, A. Godzik, Cd-hit: a fast program for clustering and comparing large sets of protein or
949 nucleotide sequences. *Bioinformatics* **22**, 1658–1659 (2006).

950 108. L. Fu, B. Niu, Z. Zhu, S. Wu, W. Li, CD-HIT: accelerated for clustering the next-generation
951 sequencing data. *Bioinformatics* **28**, 3150–3152 (2012).

952 109. M. Steinegger, J. Söding, MMseqs2 enables sensitive protein sequence searching for the analysis
953 of massive data sets. *Nat. Biotechnol.* **35**, 1026–1028 (2017).

954 110. Gene Ontology Consortium, The Gene Ontology resource: enriching a GOld mine. *Nucleic Acids*
955 *Res.* **49**, D325–D334 (2021).

956 111. D. M. Bryant, *et al.*, A Tissue-Mapped Axolotl De Novo Transcriptome Enables Identification of
957 Limb Regeneration Factors. *Cell Rep.* **18**, 762–776 (2017).

958 112. R. D. Finn, J. Clements, S. R. Eddy, HMMER web server: interactive sequence similarity
959 searching. *Nucleic Acids Research* **39**, W29–W37 (2011).

960 113. M. Punta, *et al.*, The Pfam protein families database. *Nucleic Acids Res.* **40**, D290–301 (2012).

961 114. R. D. Finn, *et al.*, The Pfam protein families database: towards a more sustainable future. *Nucleic*
962 *Acids Res.* **44**, D279–85 (2016).

963 115. T. N. Petersen, S. Brunak, G. von Heijne, H. Nielsen, SignalP 4.0: discriminating signal peptides
964 from transmembrane regions. *Nat. Methods* **8**, 785–786 (2011).

965 116. A. Krogh, B. Larsson, G. von Heijne, E. L. Sonnhammer, Predicting transmembrane protein
966 topology with a hidden Markov model: application to complete genomes. *J. Mol. Biol.* **305**, 567–580
967 (2001).

968 117. S. F. Altschul, W. Gish, W. Miller, E. W. Myers, D. J. Lipman, Basic local alignment search tool.
969 *J. Mol. Biol.* **215**, 403–410 (1990).

970 118. M. Kanehisa, S. Goto, Y. Sato, M. Furumichi, M. Tanabe, KEGG for integration and
971 interpretation of large-scale molecular data sets. *Nucleic Acids Res.* **40**, D109–14 (2012).

972 119. M. Ashburner, *et al.*, Gene ontology: tool for the unification of biology. The Gene Ontology
973 Consortium. *Nat. Genet.* **25**, 25–29 (2000).

974 120. S. Powell, *et al.*, eggNOG v3.0: orthologous groups covering 1133 organisms at 41 different
975 taxonomic ranges. *Nucleic Acids Res.* **40**, D284–9 (2012).

976 121. R. Patro, G. Duggal, M. I. Love, R. A. Irizarry, C. Kingsford, Salmon provides fast and bias-
977 aware quantification of transcript expression. *Nat. Methods* **14**, 417–419 (2017).

978 122. M. D. Robinson, D. J. McCarthy, G. K. Smyth, edgeR: a Bioconductor package for differential
979 expression analysis of digital gene expression data. *Bioinformatics* **26**, 139–140 (2010).

980 123. M. I. Love, W. Huber, S. Anders, Moderated estimation of fold change and dispersion for RNA-
981 seq data with DESeq2. *Genome Biol.* **15**, 550 (2014).

982 124. Alexa, Rahnenfuhrer, topGO: Enrichment analysis for Gene Ontology. R package version 2.28. 0.
983 *Cranio* (2016).

984 125. S. X. Ge, D. Jung, R. Yao, ShinyGO: a graphical gene-set enrichment tool for animals and plants.
985 *Bioinformatics* **36**, 2628–2629 (2020).

986 126. P. Langfelder, S. Horvath, Fast R Functions for Robust Correlations and Hierarchical Clustering.
987 *J. Stat. Softw.* **46** (2012).

988 127. Y. Mei, *et al.*, InsectBase 2.0: a comprehensive gene resource for insects. *Nucleic Acids Res.* **50**,
989 D1040–D1045 (2022).

990 128. J. Jumper, *et al.*, Highly accurate protein structure prediction with AlphaFold. *Nature* **596**, 583–
991 589 (2021).

992 129. V. Mariani, M. Biasini, A. Barbato, T. Schwede, lDDT: a local superposition-free score for
993 comparing protein structures and models using distance difference tests. *Bioinformatics* **29**, 2722–
994 2728 (2013).

995 130. B. Yariv, *et al.*, Using evolutionary data to make sense of macromolecules with a "face-lifted"
996 ConSurf. *Protein Sci.* **32**, e4582 (2023).

997 131. H. Ashkenazy, *et al.*, ConSurf 2016: an improved methodology to estimate and visualize
998 evolutionary conservation in macromolecules. *Nucleic Acids Res.* **44**, W344–50 (2016).

132. G. Celniker, *et al.*, ConSurf: Using evolutionary data to raise testable hypotheses about protein function. *Isr. J. Chem.* **53**, 199–206 (2013).

133. H. Ashkenazy, E. Erez, E. Martz, T. Pupko, N. Ben-Tal, ConSurf 2010: calculating evolutionary conservation in sequence and structure of proteins and nucleic acids. *Nucleic Acids Res.* **38**, W529–33 (2010).

134. M. Landau, *et al.*, ConSurf 2005: the projection of evolutionary conservation scores of residues on protein structures. *Nucleic Acids Res.* **33**, W299–302 (2005).

135. Schrödinger, LLC, The PyMOL Molecular Graphics System, Version 1.8 (2015).

136. N. Blom, S. Gammeltoft, S. Brunak, Sequence and structure-based prediction of eukaryotic protein phosphorylation sites. *J. Mol. Biol.* **294**, 1351–1362 (1999).

137. N. Blom, T. Sicheritz-Pontén, R. Gupta, S. Gammeltoft, S. Brunak, Prediction of post-translational glycosylation and phosphorylation of proteins from the amino acid sequence. *Proteomics* **4**, 1633–1649 (2004).

Supplemental Figures

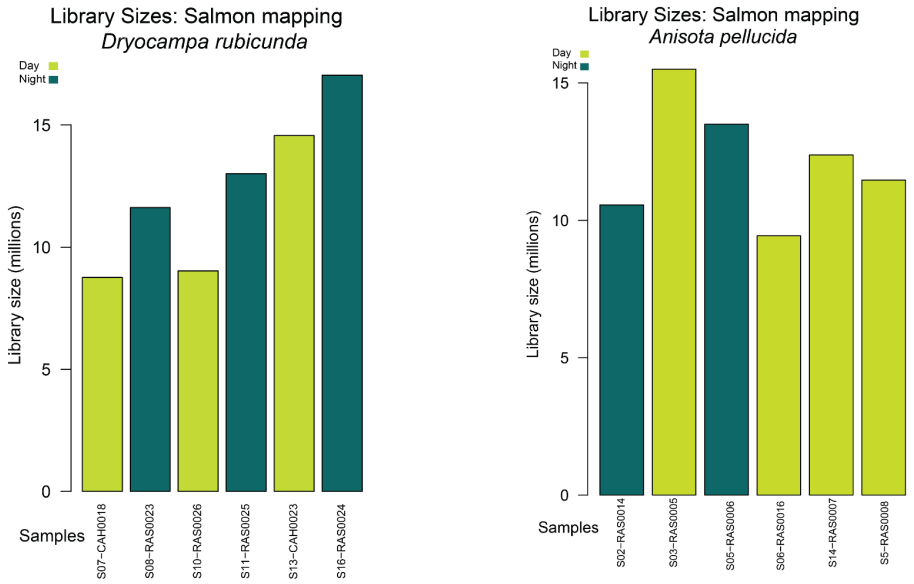

Figure S1: Variation in salmon mapped libraries for *Dryocampa rubicunda* and *Anisota pellucida*

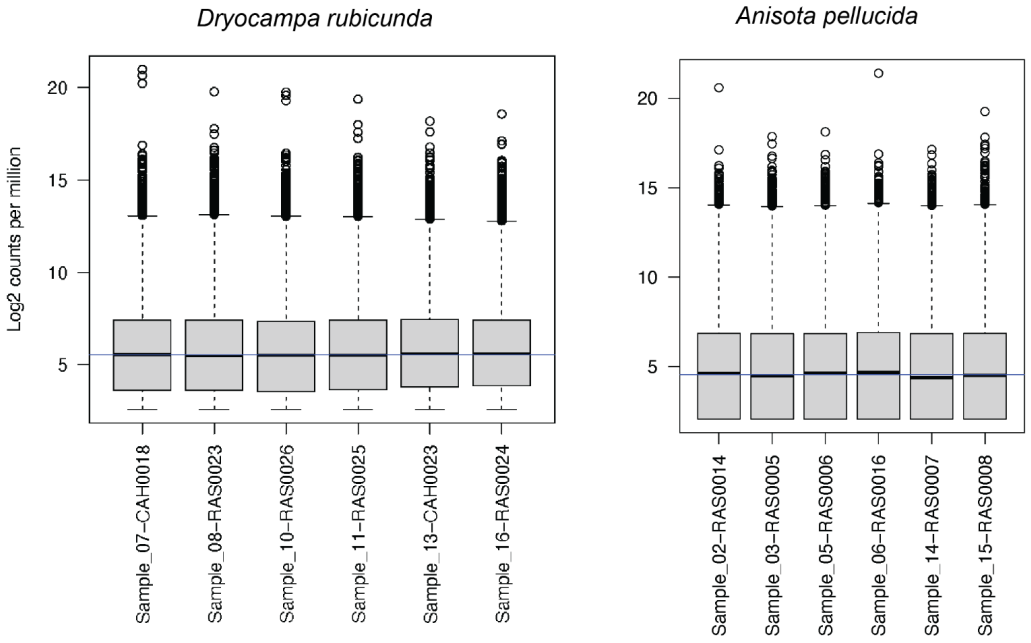

Figure S2: Variation in normalised libraries for *Dryocampa rubicunda* and *Anisota pellucida*

1039

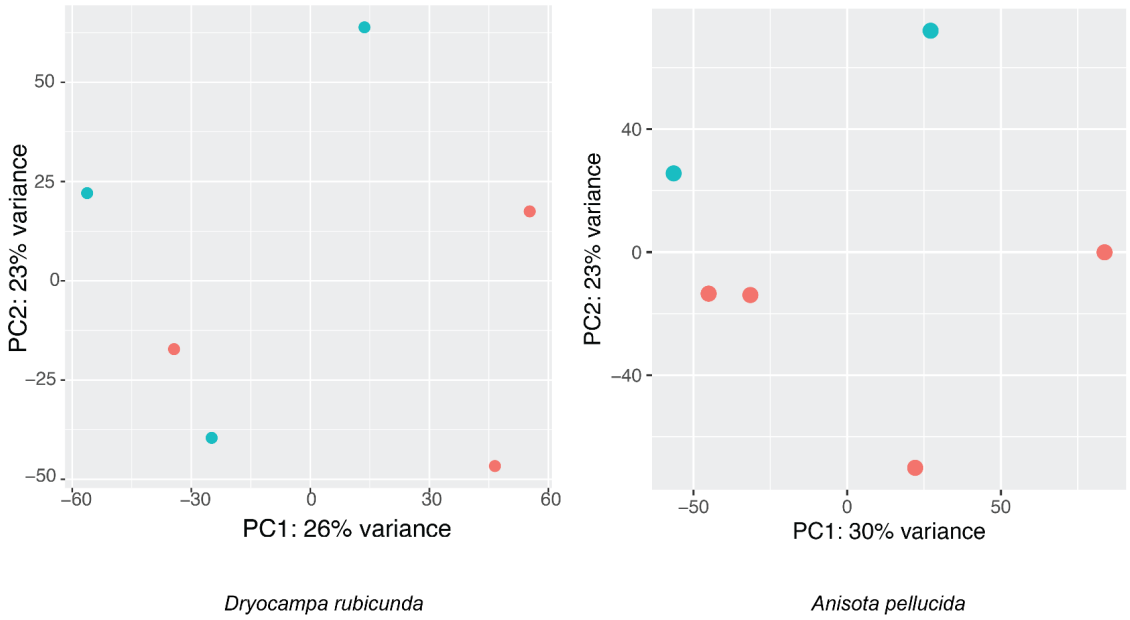

1040

1041 **Figure S3**: PC1 and PC2 of libraries labelled for *Dryocampa rubicunda* and *Anisota pellucida*.
1042 Orange and blue labels refer to midday 'Day' and midnight 'Night' collection time points,
1043 respectively. This PCA was generated from mapped salmon reads after normalising with DESeq2.

1044

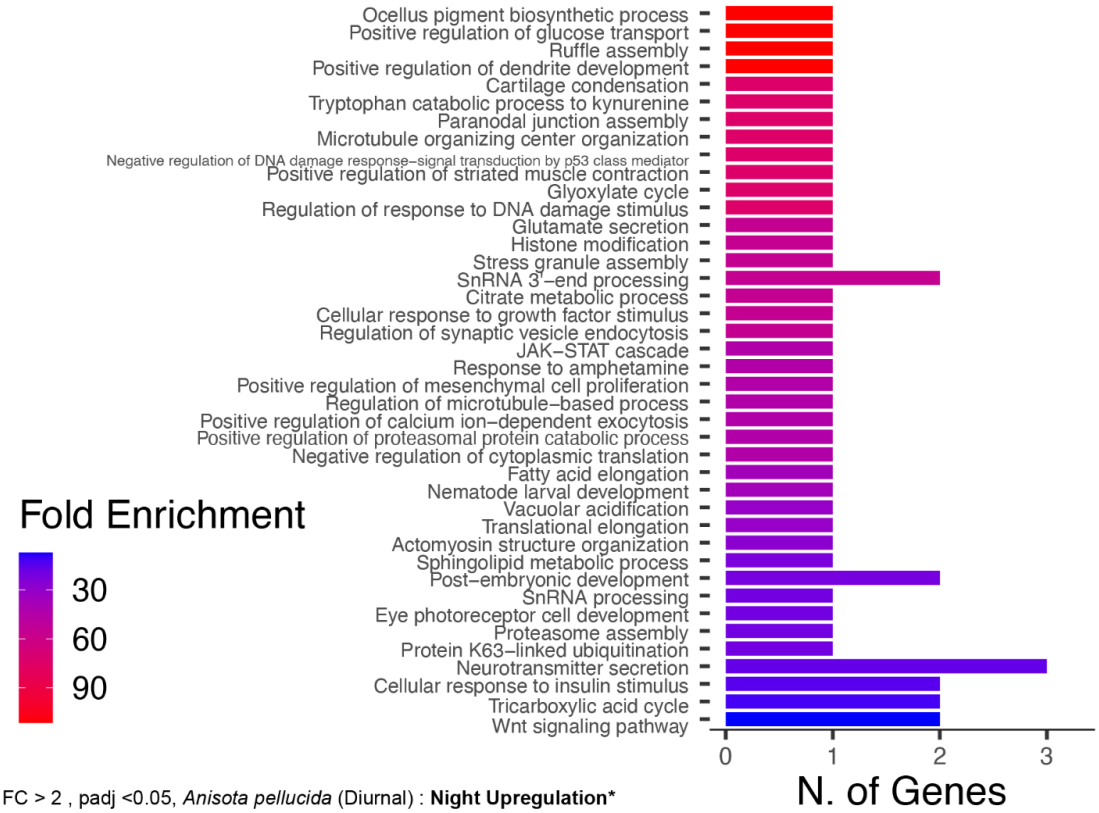

FC > 2 , padj <0.05, *Anisota pellucida* (Diurnal) : **Night Upregulation***
ShinyGO (FDR <0.1, Pathway (1-2000), top 100 pathways)

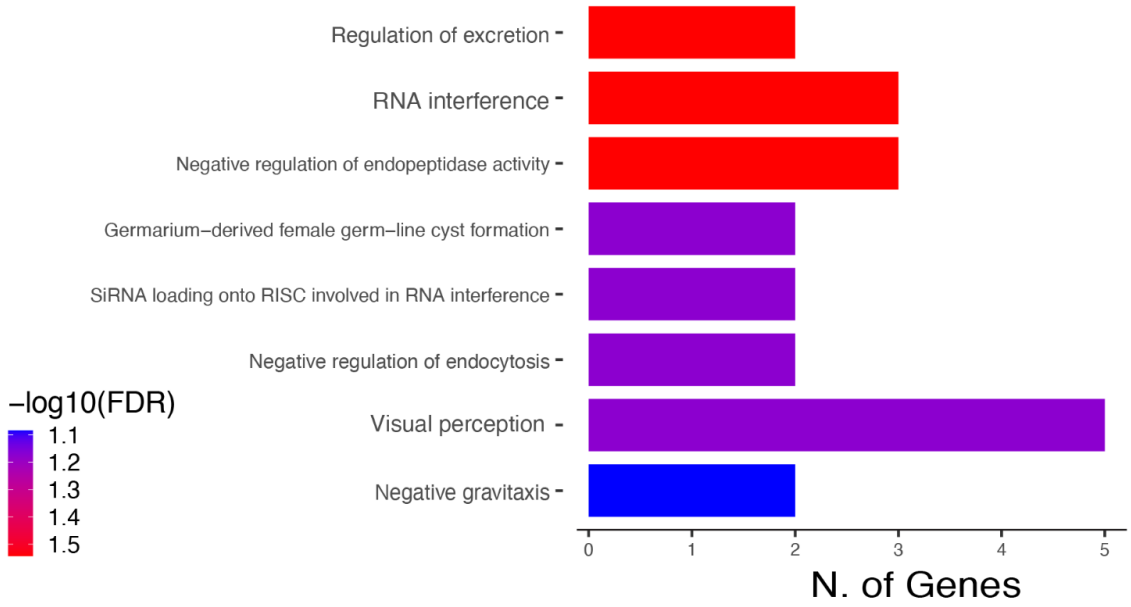

FC < -2 , padj <0.05, *Anisota pellucida* (Diurnal) : **Day Upregulation***
ShinyGO (FDR <0.1, Pathway (1-2000), top 20 pathways)

1045

1046

1047 **Figure S4**: Enriched lists of GO terms associated with significant positively and negatively
1048 expressed genes recovered from 2 or more analyses (DESeq2, WGCNA, EdgeR) for *Anisota*
1049 *pellucida.* ShinyGo was used to highlight terms with genes showing representation compared to the
1050 background of detectable genes values representing ShinyGo overrepresentation. Top: Enriched Day
1051 Upregulated genes (FDR>0.1) with gene expression FC>=2, adjusted p-value <0.05. Bottom:
1052 Enriched Night Upregulated genes (FDR>0.1) with gene expression FC<=2, adjusted p-value <0.05
1053 and that showed at least 2 occurrences in the combined dataset. Values are sorted by -log FDR
1054 *****Genes that showed up in at least 2 separate analyses are included, (>=2 occurrences in the combined
1055 dataset). The background used was all transcripts that were recovered in the DEG analysis and had
1056 *Bombyx* orthologs

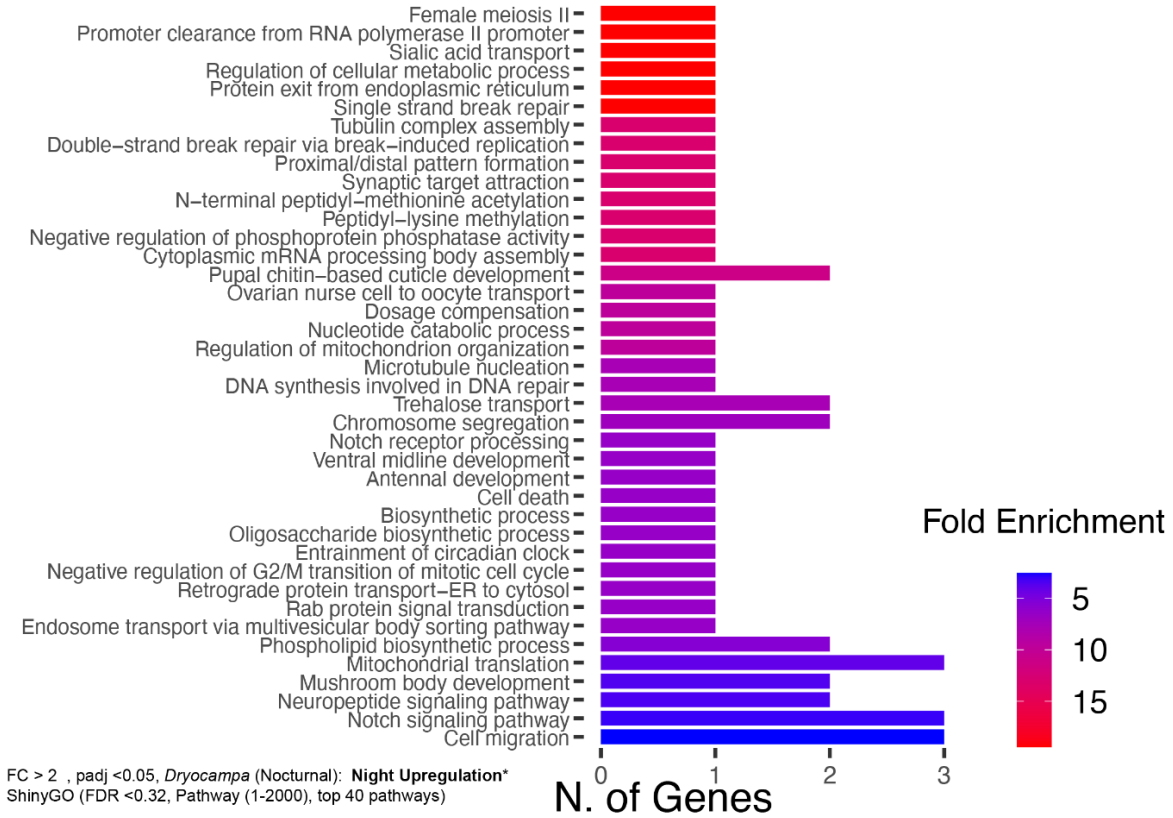
Female meiosis II
Promoter clearance from RNA polymerase II promoter
Sialic acid transport
Regulation of cellular metabolic process
Protein exit from endoplasmic reticulum
Single strand break repair
Tubulin complex assembly
Double−strand break repair via break−induced replication
Proximal/distal pattern formation
Synaptic target attraction
N−terminal peptidyl−methionine acetylation
Peptidyl−lysine methylation
Negative regulation of phosphoprotein phosphatase activity
Cytoplasmic mRNA processing body assembly
Pupal chitin−based cuticle development
Ovarian nurse cell to oocyte transport
Dosage compensation
Nucleotide catabolic process
Regulation of mitochondrion organization
Microtubule nucleation
DNA synthesis involved in DNA repair
Trehalose transport
Chromosome segregation
Notch receptor processing
Ventral midline development
Antennal development
Cell death
Biosynthetic process
Oligosaccharide biosynthetic process
Entrainment of circadian clock
Negative regulation of G2/M transition of mitotic cell cycle
Retrograde protein transport−ER to cytosol
Rab protein signal transduction
Endosome transport via multivesicular body sorting pathway
Phospholipid biosynthetic process
Mitochondrial translation
Mushroom body development
Neuropeptide signaling pathway
Notch signaling pathway
Cell migration
0
1
2
3
N. of Genes
Fold Enrichment
5
10
15
FC > 2 , padj <0.05, *Dryocampa* (Nocturnal): **Night Upregulation***
ShinyGO (FDR <0.32, Pathway (1-2000), top 40 pathways)

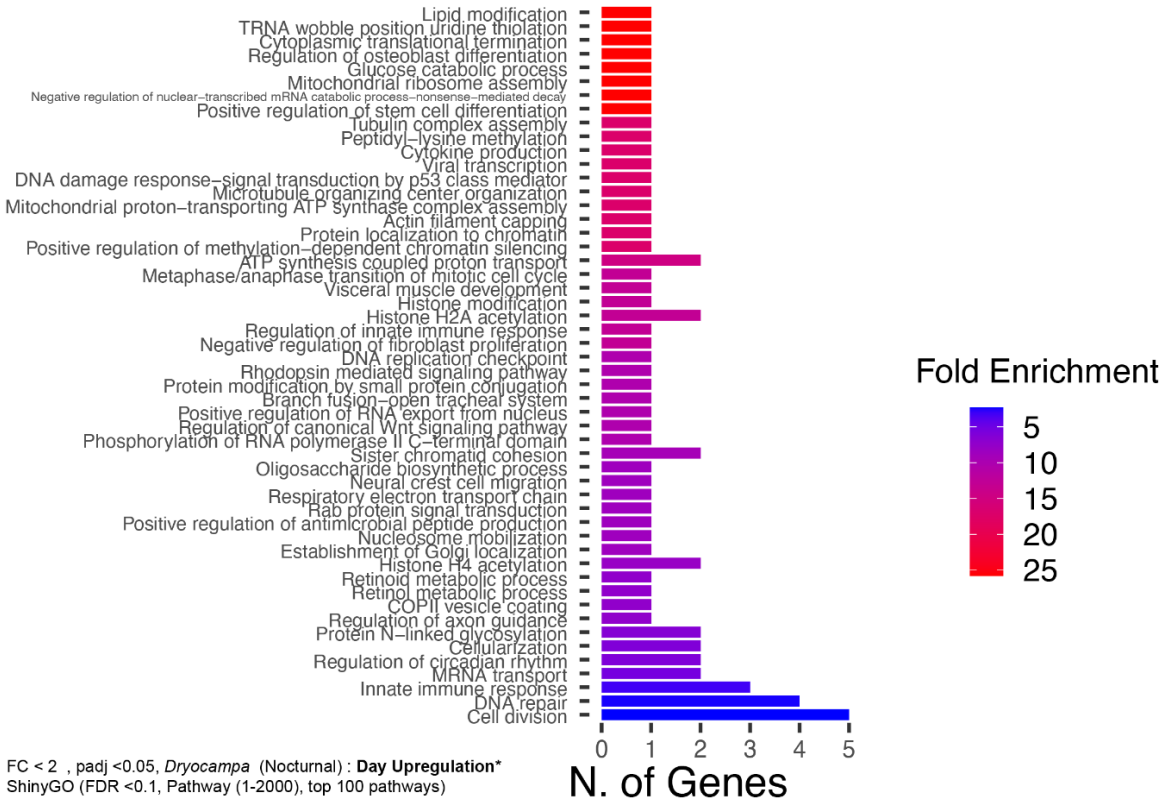
Lipid modification
TRNA wobble position uridine thiolation
Cytoplasmic translational termination
Regulation of osteoblast differentiation
Glucose catabolic process
Mitochondrial ribosome assembly
Negative regulation of nuclear−transcribed mRNA catabolic process−nonsense−mediated decay
Positive regulation of stem cell differentiation
Tubulin complex assembly
Peptidyl−lysine methylation
Cytokine production
Viral transcription
DNA damage response−signal transduction by p53 class mediator
Microtubule organizing center organization
Mitochondrial proton−transporting ATP synthase complex assembly
Actin filament capping
Protein localization to chromatin
Positive regulation of methylation−dependent chromatin silencing
ATP synthesis coupled proton transport
Metaphase/anaphase transition of mitotic cell cycle
Visceral muscle development
Histone modification
Histone H2A acetylation
Regulation of innate immune response
Negative regulation of fibroblast proliferation
DNA replication checkpoint
Rhodopsin mediated signaling pathway
Protein modification by small protein conjugation
Branch fusion−open tracheal system
Positive regulation of RNA export from nucleus
Regulation of canonical Wnt signaling pathway
Phosphorylation of RNA polymerase II C−terminal domain
Sister chromatid cohesion
Oligosaccharide biosynthetic process
Neural crest cell migration
Respiratory electron transport chain
Rab protein signal transduction
Positive regulation of antimicrobial peptide production
Nucleosome mobilization
Establishment of Golgi localization
Histone H4 acetylation
Retinoid metabolic process
Retinol metabolic process
COPII vesicle coating
Regulation of axon guidance
Protein N−linked glycosylation
Cellularization
Regulation of circadian rhythm
MRNA transport
Innate immune response
DNA repair
Cell division
0
1
2
3
4
5
N. of Genes
Fold Enrichment
5
10
15
20
25
FC < 2 , padj <0.05, *Dryocampa* (Nocturnal) : **Day Upregulation***
ShinyGO (FDR <0.1, Pathway (1-2000), top 100 pathways)

1058 **Figure S5** : Enriched lists of GO terms associated with significant positively and negatively
1059 expressed genes recovered from 2 or more analyses (DESeq2,WGCNA, EdgeR) for *Dryocampa*
1060 *rubicunda* . ShinyGo was used to highlight terms with genes showing representation compared to the
1061 background of detectable genes values representing ShinyGo overrepresentation. Top: Enriched Day
1062 Top 40 upregulated genes (FDR>0.32) with gene expression FC>=2, adjusted p-value <0.05, 77
1063 terms enriched , but not all are displayed, see supplementary material for entire list. Bottom:
1064 Enriched Night Upregulated genes (FDR>0.3) with gene expression FC<=2, adjusted p-value <0.05
1065 and that showed at least 2 occurrences in the combined dataset *Genes that showed up in at least 2
1066 separate analyses are included, (>=2 occurrences in the combined dataset). The background used was
1067 all transcripts that were recovered in the DEG analysis and had *Bombyx* orthologs
1068
1069
1070
1071
1072
1073

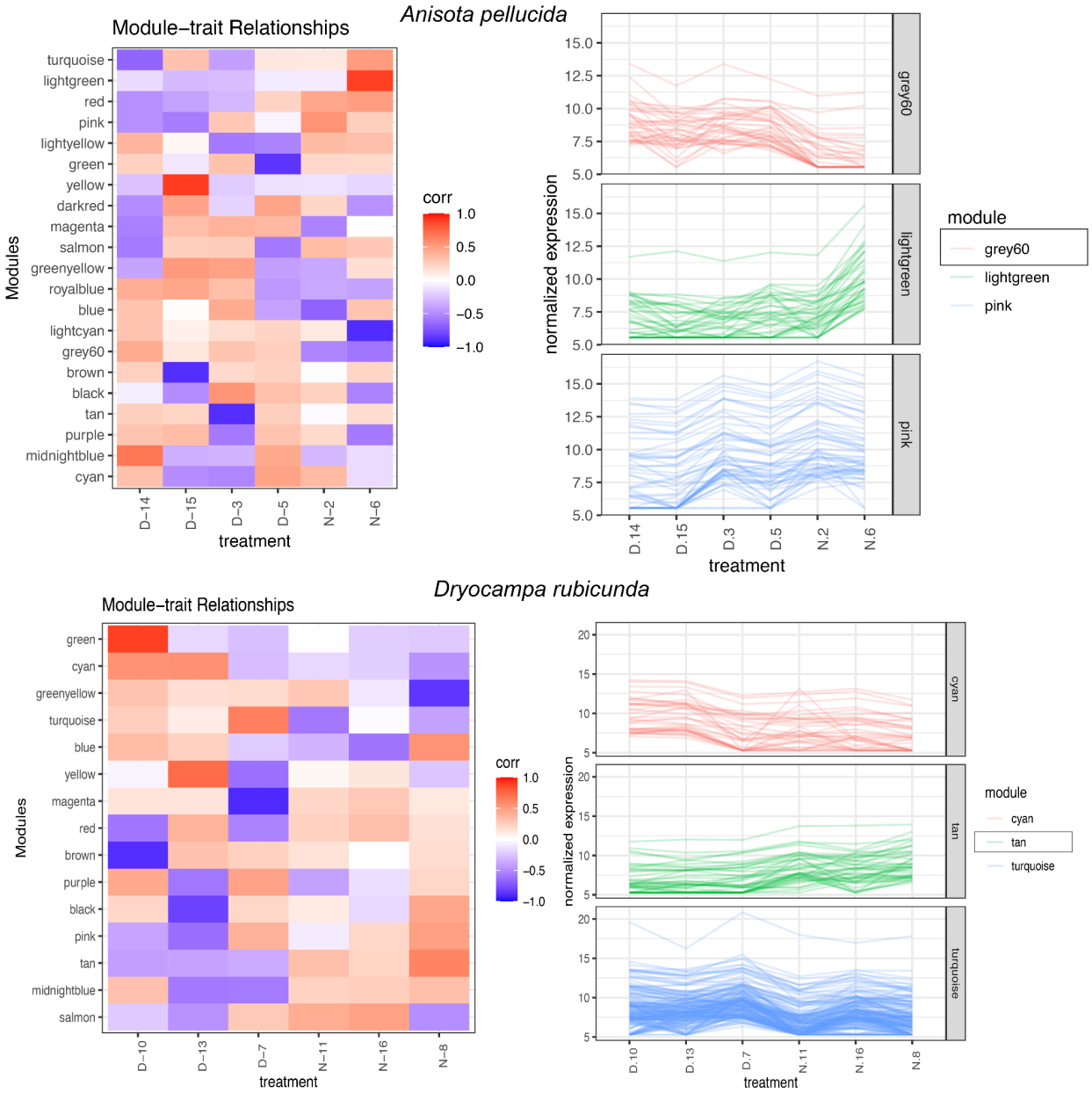

Figure S6: Modules of clustered genes grouped using normalized expression for *Anisota pellucida* (top) and *Dryocampa rubicunda* (bottom) Grey60 (38 genes) and Tan (32 genes) modules show species- time of day linked patterns. Left: Shows how patterns of gene expression correlate across samples for modules Right: Shows the normalized expression for all. Normalization was done with DESeq2 and reads were mapped to the more stringently filtered transcriptome. A soft power analysis was done and the picked power=9 for the WGCNA analysis.

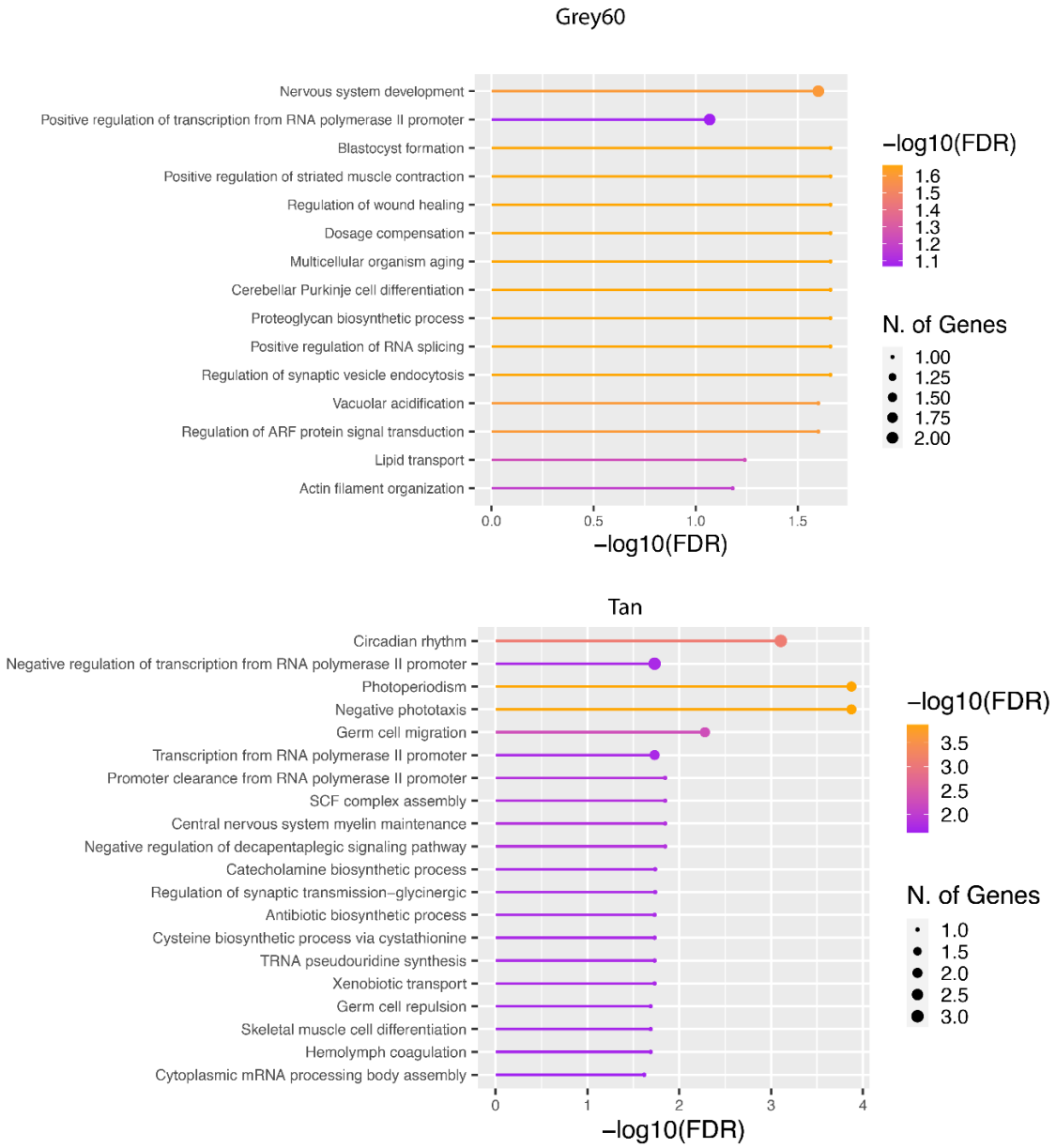

Figure S7: Shiny Go enrichment for Modules of clustered genes grouped using normalized expression for *Anisota pellucida* (top) and *Dryocampa rubicunda* (bottom) Grey60 and Tan. Background used was all *Bombyx mori* genes and FDR cut-off =0.1 min pathway =1 and GO Biological processes are displayed.

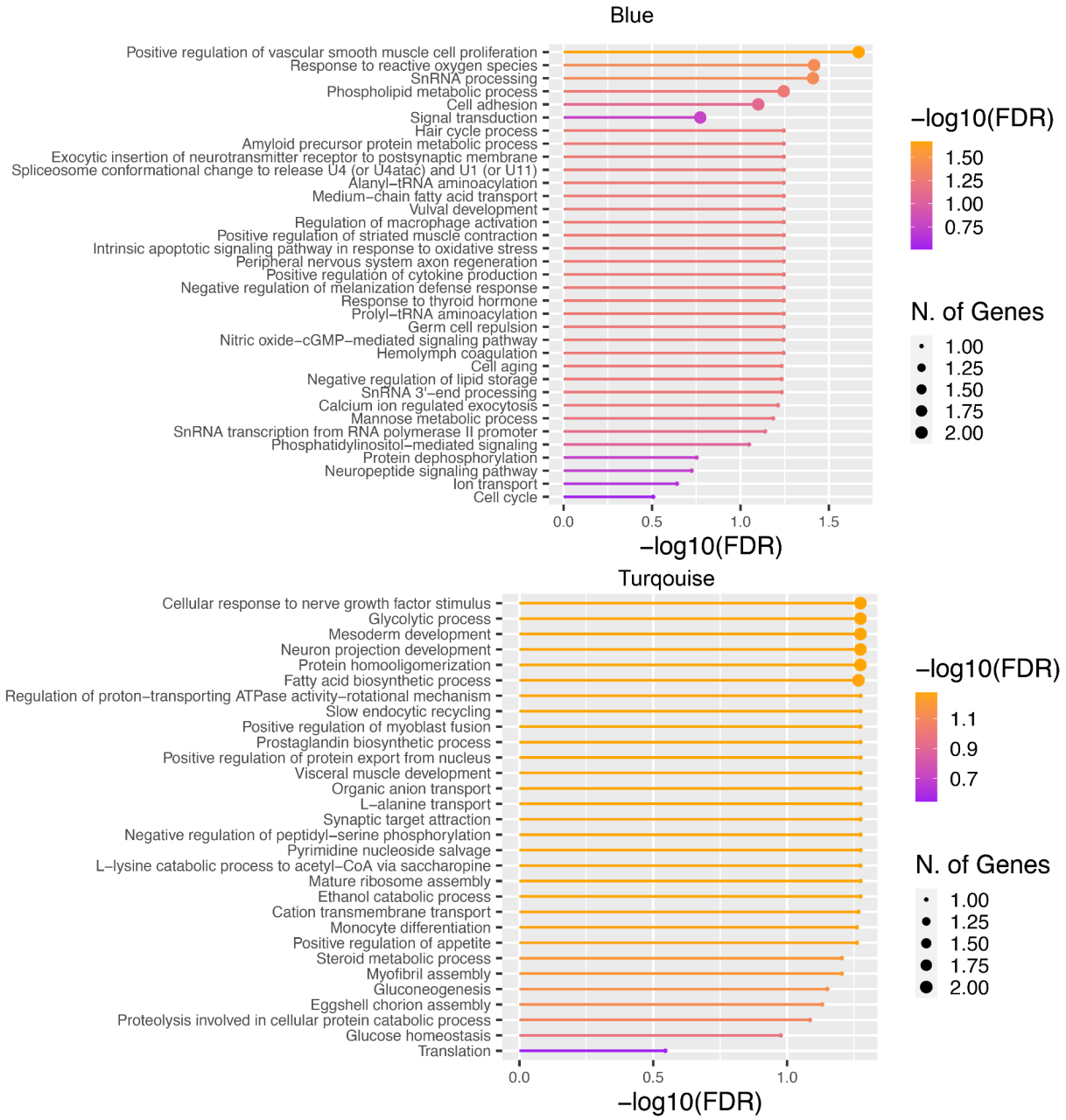

Figure S8: Shiny Go enrichment for Modules of clustered genes grouped using normalized expression for combined overlapping reads for the two species (Top) Blue and (Bottom) Turquoise. Background used was all *Bombyx mori* genes and FDR cut-off =1 min pathway =1 and GO Biological processes are displayed.

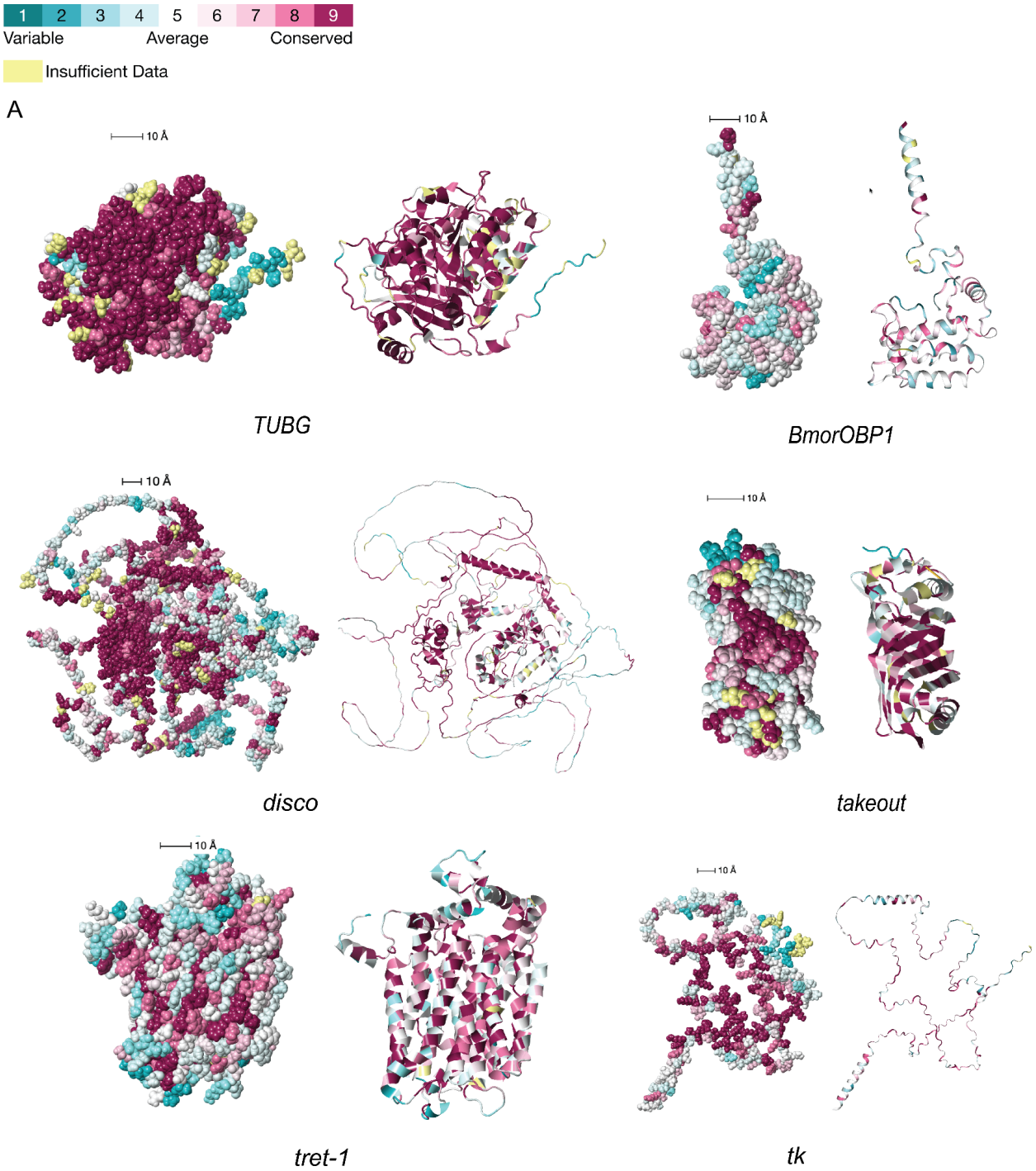

Figure S9: Variation in structural conservation across moths for predicted proteins for genes interest. Structures were obtained using AlphaFold predictions of *Bombyx mori* homologs. Left: Space filling models, Right cartoon models, colors represent conservation across the alignment from or Bombycoidea and related moth species. Conservation scores were calculated and mapped onto the

alpha fold structures using the Consurf (131) web server (For other proteins, see Supplementary data)

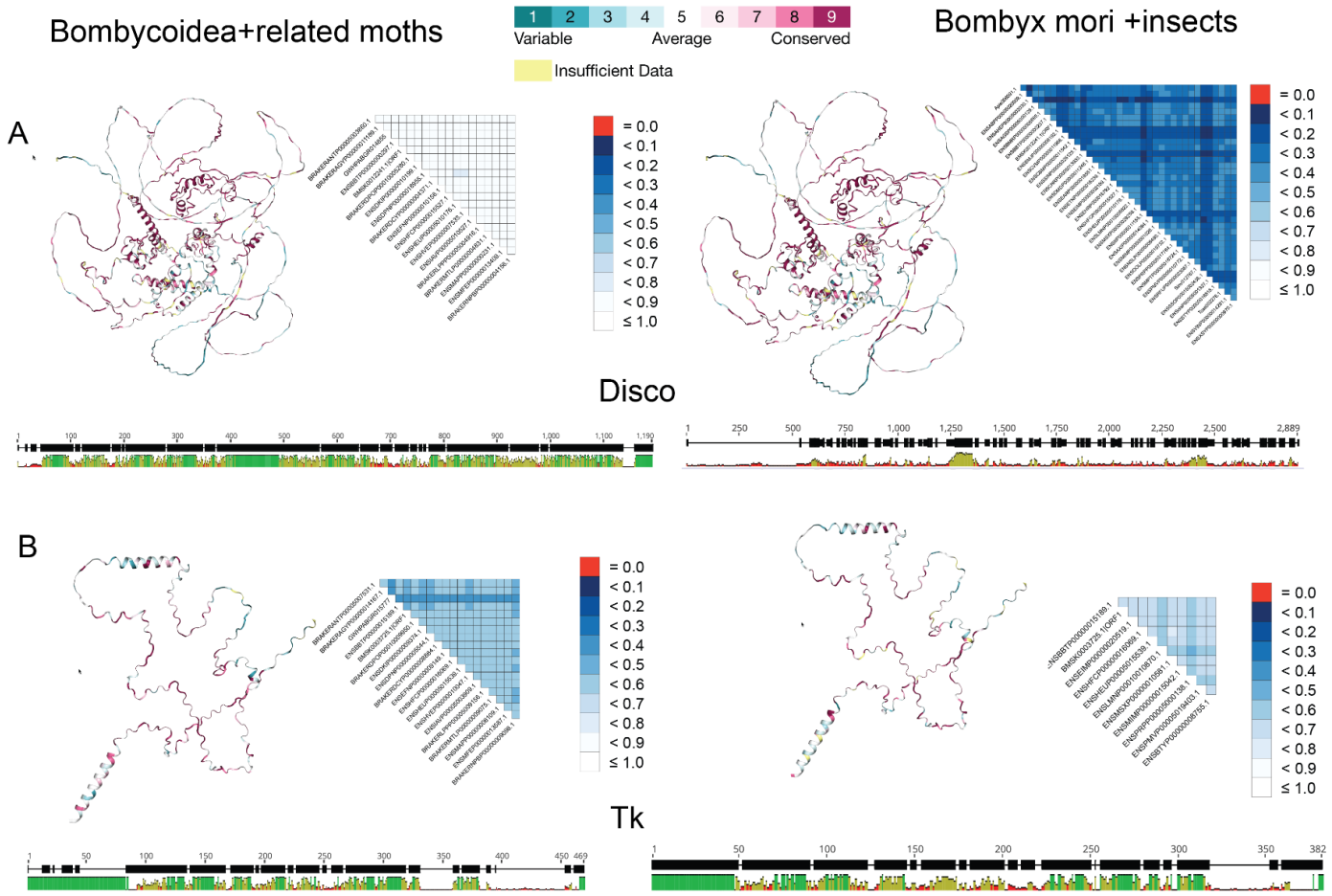

Figure S10: Illustration of conservation across the alignments and structure for **(A)** *disco* and **(B)** *tk* across Bombycoidea and relatives (Left) and insects (Right). Each inset contains the *Consurf* mapped pdb structures on the left. The *alistat* pairwise sequence conservation in the alignment scores on the right and the consensus of the protein alignments were visualized using *Geneious.* For conservation scores for other genes and lists of the species used for this modelling, see Supplementary Tales (Supp. Table: 5-7). Supplementary Dataset 10 has the associated models and output from the analyses.

Figure S11: InterPro and NetPhos predictions for *B. mori disco* protein. **(A)**InterPro predicted several zinc finger domains, disordered regions and disco and disco-related families. The numbers in black highlight the regions for the predicted domain and the numbers in red list the NetPhos predicted phosphorylated sites (threshold >0.9). **(B)** An overall distribution of the predicted phosphorylated sites with different thresholds (Left, Threshold=0.9, Right Threshold= 0.5)

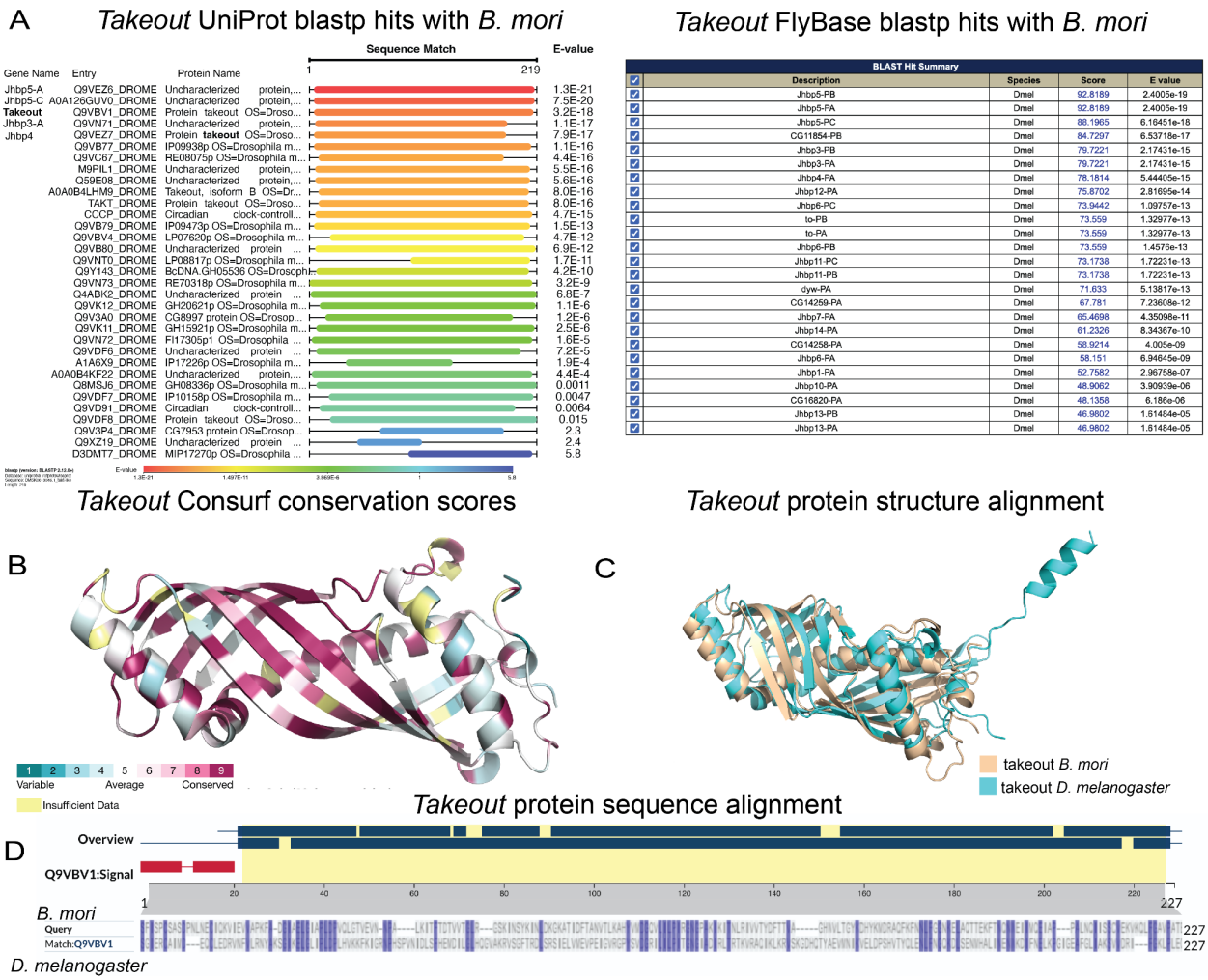

Figure S12: Lack of sequence level conservation in takeout, but high structural overlap **(A)** Right: Takeout UniProt blastp hits. (BLOSUM62, filtered for *D. melanogaster*), alignments =250, e-threshold= 10, database = uniprotkb_refprot+swissprot, list of illustrative hits is shown. Left: Similar blastp results from flybase limiting the species to *D. melanogaster.* (**B)** Consurf predicted scores for closely related moths mapped on to the *B, mori* takeout predicted protein structure. **(C)** 3D structural alignments for fly (*D. melanogaster)* and moth (*B. mori)* takeout 3D models. **(D)** Uniprot protein sequence alignment for fly and moth takeout proteins.

1132 # Tables

1133

Species	Diel-niche	Collection Time	Replicates (n)
Anisota pellucida	Diurnal	Day	4
		Night	2
Dryocampa rubicunda	Nocturnal	Day	3
		Night	3

1134

1135 **Table 1:** Sampling design showing species, collection time and number of replicates in each
1136 treatment. All specimens were male.

1137

Species	Assembler	kmer-size	Max- BUSCO groups	Lep BUSCO Score(%)	max-N50
Ani_pel	Velvet	35-85	4703 (k55)	88	3918 (k55)
Ani_pel	Soap	35-85	4682 (k35)	88.5	1661 (k35)
Ani_pel	Transabyss	35-85	4216 (k35)	79	1332 (k35)
Ani_pel	Trinity	25	4948	93	1608
Dry_rub	Velvet	45-85	4768 (k55)	90	3957 (k55)
Dry_rub	Soap	35-85	4753 (k35)	89	1915 (k75)
Dry_rub	Transabyss	55-85	3159 (k55)	59	1058 (k55)
Dry_rub	Trinity	25	4939	93	1595

1138

1139 **Table 2:** Assembly variation using different assemblers and kmer settings.

1140 Key: Dry_rub: *Dryocampa rubicunda*, Ani_pel: *Anisota pellucida.* All models included day and
1141 night samples.
1142
1143
1144
1145
1146

Species	Method	Total DEGs	DEGs (Up)	DEGs (Down)	Annotated DEGs	Unannotated %
A. pellucida D	EdgeR	350	154	196	211	39.71
D, rubicunda N	EdgeR	393	211	182	236	39.95
A. pellucida D	DESeq2	697	141	556	420	39.7
D. rubicunda N	DESeq2	498	253	245	300	39.7

1147
1148 **Table 3:** DEG recovery and gene annotation for EdgeR and DESeq2 analyses along with percent
1149 annotation using *Bombyx.* Up=FC>2, Implies night expression is greater than day expression.
1150 Down=FC<2, implies day expression is greater (control=Day, Night = Treatment)
1151

Species	Assembly annotation	BUSCO score	BUSCO duplication	No. of contigs*	Redundancy (/15k)
Dry_rub	Combined	94.3	90.8	281790	18.8x
Dry_rub	Combined_cds_cdhit_95	90.1	80.2	184808	12.3x
Dry_rub	Combined_cds_filtered (v5)	85.2	59.6	41712	2.8x
Dry_rub	Combined_cds_stringent_filter (v6)	75.4	4.9	19877	1.3x
Ani_pel	Combined	94.3	90.8	281790	18.78
Ani_pel	Combined_cds	93.9	90.3	233097	13.3x
Ani_pel	Combined_cds_filtered_cds (v5)	85.2	59.2	41712	2.8x
Ani_pel	Combined_cds_stringent_filter (v6)	79.3	4.7	19087	1.3x

1152

1153 **Table 4:** BUSCO and contig distribution statistics for different species' *de-novo* assemblies with
1154 and without filtering. Increased filtering reduces redundancy and duplication but comes at the
1155 cost of reducing BUSCO scores. *All statistics are based on contigs of size >= 500 bp.

1156

nGenes	Fold Enrichment	Pathway	GO_ID	Gene Names
2	85.53	**Regulation of excretion**	GO:0044062	NPHS1,SLC9A3R1
1	42.76	Response to herbicide	GO:0009635	Alad
1	42.76	Carbohydrate catabolic process	GO:0016052	BMSK0015853
1	42.76	Blastocyst formation	GO:0001825	Actl6a
1	42.76	Tryptophan catabolic process to kynurenine	GO:0019441	KFase
1	42.76	Microvillus assembly	GO:0030033	SLC9A3R1
1	42.76	Parallel actin filament bundle assembly	GO:0030046	jv
1	42.76	Heparan sulfate proteoglycan metabolic process	GO:0030201	botv
1	42.76	Inactivation of MAPK activity	GO:0000188	Spred1
1	42.76	B cell activation	GO:0042113	AKAP17A
1	42.76	Negative regulation of glycogen biosynthetic process	GO:0045719	Gfpt1
1	42.76	Behavioral response to pain	GO:0048266	pain
1	42.76	Interphase microtubule nucleation by interphase microtubule organizing center	GO:0051415	Grip91
1	28.51	Cellular defense response	GO:0006968	PNLIPRP2
1	28.51	Cartilage condensation	GO:0001502	COL11A1
1	28.51	Short-chain fatty acid import	GO:0015913	SLC5A8
1	28.51	Male genitalia development	GO:0030539	ken
1	28.51	Microtubule organizing center organization	GO:0031023	Gcc2
1	28.51	Telomere maintenance via semi-conservative replication	GO:0032201	RFC3
1	28.51	Glomerular basement membrane development	GO:0032836	NPHS1
1	28.51	Endosomal vesicle fusion	GO:0034058	Ankfy1
1	28.51	High-density lipoprotein particle assembly	GO:0034380	ABCA7

1	28.51	Positive regulation of Rho protein signal transduction	GO:0035025	MCF2L
1	28.51	Xenobiotic transport	GO:0042908	Mdr49
1	28.51	DNA replication-removal of RNA primer	GO:0043137	Rnaseh1
2	28.51	Negative regulation of endocytosis	GO:0045806	ABCA7,Mctp1
2	28.51	**Negative gravitaxis**	GO:0048060	pain,pyx
1	28.51	Imaginal disc-derived wing expansion	GO:0048526	Spn88Ea
1	28.51	**Positive regulation of synapse structural plasticity**	GO:0051835	FRMPD4
1	28.51	Chitin biosynthetic process	GO:0006031	chs-2
2	19.01	Lysosomal transport	GO:0007041	Vps53,g
2	19.01	RNA interference	GO:0016246	Dcr-1,bel
2	15.55	Negative regulation of endopeptidase activity	GO:0010951	Spn88Ea,Serpinb1a
2	13.16	Formation of cytoplasmic translation initiation complex	GO:0001732	eIF3-S5, BMSK0008517
2	10.69	Protein heterotetramerization	GO:0051290	pyx,Agrn
2	10.06	**Positive regulation of synaptic growth at neuromuscular junction**	GO:0045887	Agrn,Sin1
2	8.55	Endoplasmic reticulum organization	GO:0007029	atl,Lman1
2	7.78	**Regulation of synaptic growth at neuromuscular junction**	GO:0008582	atl,hiw
2	7.13	Negative regulation of cell migration	GO:0030336	SLC9A3R1,Mctp1
5	5.94	**Visual perception**	GO:0007601	RDH11,COL11A1, OP1,WDR36,disco

Table 5: Top significantly enriched GO terms for *A. pellucida* day upregulation

No. Genes	Fold Enrichment	Pathway	GO_ID	Gene Names
1	41.61	Female meiosis II	GO:0007147	polo
1	41.61	Female germline ring canal formation-actin assembly	GO:0008302	Src64B
1	41.61	Dosage compensation by hyperactivation of X chromosome	GO:0009047	mle
1	41.61	10-formyltetrahydrofolate catabolic process	GO:0009258	aldh1l1
1	41.61	**Sialic acid transport**	**GO:0015739**	**SLC17A5**

1	41.61	Arachidonic acid metabolic process	GO:0019369	FAAH2
1	41.61	Regulation of cellular metabolic process	GO:0031323	melt
1	41.61	Protein exit from endoplasmic reticulum	GO:0032527	SEC16A
1	41.61	Single strand break repair	GO:0000012	gkt
1	41.61	Ring gland development	GO:0035271	gl
1	41.61	Notch receptor processing-ligand-dependent	GO:0035333	Nct
1	41.61	Positive regulation of RNA polymerase II transcriptional preinitiation complex assembly	GO:0045899	PSMC6
1	41.61	Tetrahydrofolate metabolic process	GO:0046653	MTHFS
1	41.61	Neurotrophin TRK receptor signaling pathway	GO:0048011	Bcar1
1	41.61	Glucose catabolic process	GO:0006007	agp
1	41.61	Glutaminyl-tRNAGln biosynthesis via transamidation	GO:0070681	gatA
1	41.61	Error-free translesion synthesis	GO:0070987	POLH
1	41.61	Protein deubiquitination involved in ubiquitin-dependent protein catabolic process	GO:0071947	trbd
1	41.61	Negative regulation of release of cytochrome c from mitochondria	GO:0090201	Parl
1	41.61	Regulation of cardiac conduction	GO:1903779	nkx-2.5
1	41.61	Methionyl-tRNA aminoacylation	GO:0006431	MetRS-m
2	33.29	Tetrahydrofolate interconversion	GO:0035999	Sardh,MTHFS
1	27.74	Tubulin complex assembly	GO:0007021	Tbcd
1	27.74	Double-strand break repair via break-induced replication	GO:0000727	Cdc45
1	27.74	Aminophospholipid transport	GO:0015917	ATP11B
1	27.74	**Synaptic target attraction**	**GO:0016200**	**Ten-a**
1	27.74	N-terminal peptidyl-methionine acetylation	GO:0017196	Naa60
1	27.74	Peptidyl-lysine methylation	GO:0018022	Eef1akmt2
1	27.74	Negative regulation of ossification	GO:0030279	LRP4
1	27.74	Negative regulation of phosphoprotein phosphatase activity	GO:0032515	Bod1
1	27.74	Store-operated calcium entry	GO:0002115	olf186-F
1	27.74	Cytoplasmic sequestering of transcription factor	GO:0042994	Sufu
1	27.74	Melanin biosynthetic process from tyrosine	GO:0006583	BMSK0009475
1	20.80	Cytoplasmic mRNA processing body assembly	GO:0033962	patl1

1	20.80	Positive regulation of transcription from RNA polymerase I promoter	GO:0045943	HEATR1
1	20.80	Negative regulation of insulin secretion	GO:0046676	HADH
1	16.64	Microtubule nucleation	GO:0007020	TUBG1
1	16.64	**Eclosion rhythm**	**GO:0008062**	**disco**
1	16.64	Late endosome to vacuole transport	GO:0045324	chmp3
1	16.64	**Negative regulation of axon extension involved in axon guidance**	**GO:0048843**	**tap**
1	16.64	Glucose transmembrane transport	GO:1904659	SLC2A3
1	16.64	Nucleocytoplasmic transport	GO:0006913	Anp32a
2	13.87	Chromosome segregation	GO:0007059	PPP2R1A,Naa60
1	13.87	Nucleotide catabolic process	GO:0009166	BMSK0009399
1	13.87	Phosphatidylethanolamine biosynthetic process	GO:0006646	PCYT2
2	12.80	Negative regulation of sequence-specific DNA binding transcription factor activity	GO:0043433	melt,Sufu
2	10.40	Protein heterotetramerization	GO:0051290	pyx,LRP4
2	9.25	Phospholipid biosynthetic process	GO:0008654	Mboat1,PCYT2
2	9.25	**Locomotor rhythm**	**GO:0045475**	**Ork1,disco**
2	8.76	Pupal chitin-based cuticle development	GO:0008364	Gld,Gld
3	8.61	Mitochondrial translation	GO:0032543	BMSK0007759,MRPS35,gatA
2	8.32	Sperm storage	GO:0046693	Gld,Gld
2	7.93	Cytoplasmic translation	GO:0002181	RpL4,
2	7.93	Synaptic growth at neuromuscular junction	GO:0051124	LRP4,Ten-a
2	7.56	Negative regulation of canonical Wnt signaling pathway	GO:0090090	PSMC6,LRP4
2	6.93	**Mushroom body development**	**GO:0016319**	**tap,Src64B**
2	6.93	Post-translational protein modification	GO:0043687	TULP4,PSMC6
2	6.93	**Synapse organization**	**GO:0050808**	**Ten-a,LRP4**
2	5.74	**Trehalose transport**	**GO:0015771**	**Tret1-1,Tret1-1**
2	5.20	Positive regulation of canonical Wnt signaling pathway	GO:0090263	PSMC6,trbd
3	5.09	Cell migration	GO:0016477	trbd,Bcar1,SPEF1
2	5.04	Response to endoplasmic reticulum stress	GO:0034976	SEC16A,Pdi

3	4.62	Mitotic cell cycle	GO:0000278	TUBG1,Tbcd,polo
2	4.62	Microtubule cytoskeleton organization	GO:0000226	TUBG1,Tbcd
3	3.37	G-protein coupled receptor signaling pathway	GO:0007186	Bcar1,Atrnl1,TRHR

1160

1161 **Table 6:** Top significantly enriched GO terms for *D. rubicunda* night upregulation

1162

1163

1164

Gene Symbol	Gene Name	Function	DESeq2	EdgeR	WGCNA	Flybase ID	SILKD ID
BNC1/disco	disconnected	vision	1*	1*		FBgn0000459	BMSK0012241
Spt5	Spt5	transcription	1*	1*		FBgn0040273	BMSK0011143
1q/trbd	trabid	development		1		FBgn0037734	BMSK0015294
RpL4	Ribosomal protein L4	energy use, Ribosomal production	1*			FBgn0003279	BMSK0006059
Prp2/PPO2	Prophenoloxidase 2	Wound melanization	1*			FBgn0033367	BMSK0009475
mRpS5	mitochondrial ribosomal proteins	energy use, mitochondrial maintenance	1*			FBgn0287187	BMSK0014662
SLC2A6/Tret1-1	Solute Carrier Family 2 Member 6	locomotion, energy metabolism	1*			FBgn0050035	BMSK0003817**, BMSK0003818
TUBG1/γTub23C	tubulin gamma 1	brain development in adult	1*			FBgn0260639	BMSK0002451
PARL/rho-7	presenilin associated rhomboid like	mitochondrial maintenance	1*			FBgn0033672	BMSK0008635
SLC17A5/MFS10	Solute carrier family 17 member 5	transmembrane ion transporter	1*			FBgn0030452	BMSK0001219
titin1/sls	sallimus	locomotion	1			FBgn0086906	BMSK0000202
unc-22/unc	uncoordinated	adult locomotion, hearing	1		1	FBgn0003950	BMSK0015609**, BMSK0000066
ARHGAP17/ RhoGAP92B	rho GTPase-activating protein 17	auditory, brain development			1	FBgn0038747	BMSK0009977
tk	tachykinin	locomotion and circadian rhythms			1	FBgn0037976	BMSK0003725
BmorOBP1/	Odorant Binding	odor binding			1	FBgn0034768	BMSK0013390

Obp58a	Protein 1						
PPAP2A/wun	Inorganic Pyrophosphatase 2/ wunnen	vision			1	FBgn0016078	BMSK0011305
BmorOBP2/ Obp84a	Odorant Binding Protein 2	odor binding			1	FBgn0011282	BMSK0009610
takt/JHBP	takeout-like	circadian			1	FBgn0038395	BMSK0013046

Table 7: Gene symbol from EggNog or *B. mori* annotation. Gene names, function and closest flybase ID orthologs used to collect evidence for the various listed functions.* Indicated that the gene altered direction or trend of expression across a diel pair. ** Indicates this ortholog was used for structural modeling and conservation analyses. This list is only a subset of the genes recovered from various analyses. The genes were chosen because they had either 1) multiple lines of evidence, robust divergent expression pattern, or 2) a gene ontology term for sensory or circadian function among three datasets. For exhaustive lists, see Supplementary Data

Process	**Search Query**	**Excluding**
Vision	"vision" or "eye" or "visual" or " compound eye" or "visual perception" or "light" or "ocellus" or "visual" or "photoreceptor"	- "chain" -"immunoglobulin" -"light harvesting" -"photosynthesis" -"plastid" -"plant" -actin -myosin -photoperiod -touch -smell -"light chain"
Smell	"olfaction" or "smell" or "antennal" or "olfactory" or "odor" or "pheromone"	
Hearing	"audition" or "hearing" or "sound" or "auditory" or "tympanum" or "ear"	

Circadian	"circadian" or "rhythm" or "clock" or "diurnal" or "nocturnal" or "entrainment"	
Behaviour	"locomotion" or "flight" or "behavioral"	- "cell" - "morphogenesis" - "development" or - "pheromone"
Brain	"neural plasticity" or "brain" or "neuropeptide"	

Table 8: GO query terms for functional lookup